

**On the Use of Wind Power and Pumped-Storage Hydro for Blackout
Restoration and Resilience**

by Jinshun Su

B.S. in Electrical Engineering, July 2017, Xi'an University of Technology

A Thesis submitted to

The Faculty of
The School of Engineering and Applied Science
of The George Washington University
in partial fulfillment of the requirements
for the degree of Master of Science

May 19, 2019

Thesis directed by

Payman Dehghanian
Assistant Professor of Engineering and Applied Science

© Copyright 2019 by Jinshun Su
All rights reserved

Dedication

I would like to dedicate my thesis to my parents and grandparents who always fully supported me in high education.

Acknowledgments

I would like to express my sincere gratitude to my advisor, Prof. Payman Dehghanian, for his understanding, wisdom, patience, encouragements, and for pushing me farther than where I thought I could go. His guidance and feedback helped me in all the time of courses, research and writing of this thesis.

I also want to thank to my committee members, Prof. Robert J. Harrington and Prof. Milos Doroslovacki, for their time, guidance, and exquisite support throughout the course of this Master research.

Appreciation goes to my friends and the GW SmartGrid Laboratory members, especially Bo Wang, Shiyuan Wang, Mohannad Alhazmi, Mostafa Nazemi, Li Li, Zijiang Yang, Bhavesh Shinde, and the department faculty and staff for making my time at George Washington University a wonderful experience in a healthy and friendly environment.

Most of all, I am fully grateful to my parents and grandparents for terrific supports, which are more than words can describe.

Abstract

On the Use of Wind Power and Pumped-Storage Hydro for Blackout Restoration and Resilience

Recently, natural disasters causing huge damages occur more frequently than ever before, and the electricity outages and blackouts potentially become more commonplace. It is necessary to develop an efficient and effective restoration strategy for ameliorating the grid-scale capability of restoration. With the increasing penetration of wind energy, wind power generators will play more and more important role on the system operation and restoration. In addition, due to their flexible characteristics, pumped-storage hydro (PSH) units can absorb redundant power from the system and assist in system operation or the restoration process during emergencies by supplying power into the system as needed.

This thesis focuses on designing an optimal restoration strategy through the effective coordination of wind energy and PSH. A new optimization model for power grid restoration in the face of emergencies is established. The formulation can determine the generator start-up and transmission recovery sequence. With the participation of wind energy and PSH, the total load pickup significantly increases much faster than the base case scenario without such technologies during the restoration period. The model runs in the GAMS optimization environment and is a mixed-integer linear programming formulation; the developed strategy is comprehensively tested on the modified IEEE 57 bus test system where the numerical results illustrate that the coordination of wind energy and PSH can significantly increase the load pickup and shorten the outage restoration time, thereby enhancing the grid resilience, and also reduce wind power curtailment.

Table of Contents

Dedication	ii
Acknowledgments	iii
Abstract.....	iv
Table of Contents	v
List of Figure	viii
List of Table.....	x
Nomenclature	xi
Chapter 1: Introduction	1
1.1 Background.....	1
1.2 General Review for Restoration.....	3
1.3 Research Motivation	6
1.4 Thesis Outline	8
Chapter 2: Literature Review.....	11
2.1 Introduction	11
2.2 Application of the Black-Start Generating Units for Restoration.....	11
2.3 The Application of Renewable Resources for Restoration.....	14
2.4 Other Techniques for Restoration	17
2.4.1 Topology Control for Restoration.....	17
2.4.2 Energy Storage for Restoration.....	18
2.4.3 Other Paradigms for Recovery and Resilience.....	19
Chapter 3: Formulations for System Restoration under the Base Case Scenario	20
3.1 Introduction	20
3.2 Problem Formulation.....	20
3.2.1 Initial Conditions Constraints	22
3.2.2 Energization Sequence Constraints	23
3.2.3 Components Characteristics Constraints.....	25
3.2.4 Power balance constraints	26
3.2.5 Load Pickup Constraints	28
3.3 Case Study.....	28
3.3.1 Optimal Generator Start-up Sequence.....	29
3.3.2 Optimal Transmission Re-energization Path.....	30

3.4 Conclusion.....	37
Chapter 4: Incorporating Wind Energy in Power System Restoration.....	39
4.1 Introduction.....	39
4.2 Problem Formulation.....	39
4.2.1 Initial Conditions Constraints.....	40
4.2.2 Energization Sequence Constraints.....	40
4.2.3 Components Characteristics Constraints.....	41
4.2.4 Power Balance Constraints.....	41
4.2.5 Load Pickup Constraints.....	42
4.3 Case Study.....	42
4.4 Sensitivity Analysis.....	44
4.4.1 Impact of Wind Power Penetration.....	44
4.4.2 The Impact of the Wind Farm's Location.....	46
4.4.3 The Impact of Wind Farms' Quantity.....	49
4.5 Conclusion.....	51
Chapter 5: Coordination of Wind Power and PSH for System Restoration.....	53
5.1 Introduction.....	53
5.2 Problem Formulation.....	54
5.2.1 Initial Conditions Constraints.....	54
5.2.2 Energization Sequence Constraints.....	55
5.2.3 Components Characteristics Constraints.....	55
5.2.4 Power Balance Constraints.....	55
5.2.5 Load Pickup Constraints.....	56
5.2.6 PSH Constraints.....	56
5.3 Case Study.....	57
5.3.1 Case 1.....	57
5.3.2 Case 2.....	60
5.3.3 Case 3.....	61
5.4 Conclusion.....	65
Chapter 6: Conclusion.....	67
6.1 Conclusion.....	67
6.2 Suggestions for Future Research.....	68

References	70
Appendix 1: Linearized AC Power Flow Model	83
Appendix 2: Data of IEEE 57 Bus System.....	85
Appendix 3: Data of Pumped-Storage Hydro	88

List of Figure

Figure 1 Significant weather-related U.S. electric grid disturbances [4].....	2
Figure 2 Restoration Process [28].....	4
Figure 3 Coordinated frequency control for WPG participation in the BS procedure [64]	16
Figure 4 BS Restoration Process	21
Figure 5 Illustration of logical sequences for transmission path	23
Figure 6 IEEE 57 Bus system	29
Figure 7 (a)~(l) Transmission restoration path from 1 p.u. time to 12 p.u. time	36
Figure 8 Total generated power and real and reactive load pickup in the base case scenario	37
Figure 9 Modified IEEE 57-bus test system with a wind farm.....	42
Figure 10 Total load pickup in the case with wind farm at bus 38.....	44
Figure 11 Total load pickup with different wind penetration levels.....	45
Figure 12 (a) ~ (d) Wind power with different penetration of wind farms.....	46
Figure 13 Total load pickup at different location of the wind farm.....	47
Figure 14 (a) ~ (d) Wind farm power at different locations	48
Figure 15 Total load pickup with different number of wind farms	50
Figure 16 (a) ~ (c) Wind power with different number of wind farms.....	51
Figure 17 Typical configuration of a pumped storage hydropower plant [131].....	53
Figure 18 Modified IEEE 57-bus test system with a PSH located at bus 38.....	58
Figure 19 Total load pickup with PSH located at bus 38	59
Figure 20 Forecasted and scheduled wind power in Case 1	59

Figure 21 Reservoir volume of PSH.....	60
Figure 22 Forecasted and scheduled wind power in Case 2	61
Figure 23 Modified IEEE 57-bus system with PSH located at bus 29	62
Figure 24 Total load pickup in Case 3	64

List of Table

Table 1 Optimal Start-up Time for Generators.....	29
Table 2 Cranking Power Supply Path.....	29
Table 3 The Amount of Demand Loads at Each Time Step.....	30
Table 4 The Amount of Pickup Loads at Each Time Step in the Case with Wind.....	43
Table 5 Operating Modes of PSH in Case 1	59
Table 6 Operating Modes of PSH in Case 2.....	61
Table 7 Optimal Start-up Time for Generators.....	63
Table 8 Energized Time of all Buses	63
Table 9 Energized Time of all Transmission Lines	63
Table 10 The Amount of Pickup Loads at Each Time Step in Case 3.....	64
Table 11 Operating Modes of PSH in Case 3.....	65
Table 12 Generator Characteristics.....	85
Table 13 Load Data and Priorities	85
Table 14 Transmission Lines Data	86
Table 15 PSH Units' Characteristics	88

Nomenclature

Nomenclature 1: Chapter 3

A. Sets

- $t \in T$ Set of restoration times.
- $g \in G$ Set of all generating units.
- $g \in G_{BS}$ Set of black-start generating units.
- $g \in G_{NBS}$ Set of non-black-start generating units.
- $d \in D$ Set of load demands.
- $i, j \in B$ Set of transmission buses.
- $i \in B_{BS}$ Set of buses connected to the black-start generating unit g .
- $i \in B_{NBS}$ Set of buses connected to the non-black-start generating unit g .
- $i \in B_k$ Set of buses connected to transmission line k .
- $i \in B_d$ Set of system load points.
- $k \in K$ Set of transmission lines.
- $k \in K_i$ Set of transmission lines connect to bus i .
- $k \in K_f$ Set of transmission lines with the sending end as bus i .
- $k \in K_r$ Set of transmission lines with receiving end as bus i .

B. Decision Variables

- $n_{g,t}$ Binary variable equal to 0/1 if generating unit g is off/on at time t .
- $n_{g,t}^{start}$ Binary variables equal to 0/1 if generating unit g is out/in start-up period.

$n_{i(j),t}$	Binary variables equal to 0/1 if bus i/j is de-energized/energized at time t .
$n_{k,t}$	Binary variables equal to 0/1 if line k is de-energized/energized at time t .
$P_{d,t}$	Amount of real restored load at the load point d at time t .
$Q_{d,t}$	Amount of reactive restored load at the load point d at time t .
$P_{g,t}$	Scheduled real power of generating unit g at time t .
$Q_{g,t}$	Scheduled reactive power of generating unit g at time t .
$P_{g,t}^{start}$	Cranking power of generating unit g at time t .
$P_{k,t}$	Real power flow in transmission line k at time t .
$Q_{k,t}$	Reactive power flow in transmission line k at time t .
$V_{i(j),t}$	Bus voltage magnitude in p.u. at bus i/j at time t .
$\Delta V_{i(j),t}$	Bus voltage magnitude deviation from 1 p.u. at bus i/j at time t .
$\theta_{k,t}$	Phase angle difference across transmission line k .

C. Parameters

P_g^{\max}	Maximum real power capacity of generating unit g .
P_g^{\min}	Minimum real power capacity of generating unit g .
Q_g^{\max}	Maximum reactive power capacity of generating unit g .
Q_g^{\min}	Minimum reactive power capacity of generating unit g .
P_g^{start}	Cranking power of generating unit g .
P_d^{\max}	Maximum restorable real load at load point d .

P_d^{\min}	Minimum restorable real load at load point d .
Q_d^{\max}	Maximum restorable reactive load at load point d .
Q_d^{\min}	Minimum restorable reactive load at load point d .
P_k^{\max}	Maximum real power limit of transmission line k .
P_k^{\min}	Minimum real power limit of transmission line k .
Q_k^{\max}	Maximum reactive power limit of transmission line k .
Q_k^{\min}	Minimum reactive power limit of transmission line k .
$\hat{\partial}_d$	Priority factor of demand d .
T_s	Start-up duration of generating unit g .
RR_g	Ramp rate of generating unit g .
b_k	Series admittance of transmission line k .
b_{k0}	Shunt admittance of transmission line k .
g_k	Conductance of transmission line k .
λ_g	Load pickup factor of generating unit g .

Nomenclature 2: Chapter 4

A. Sets

$w \in W$	Set of wind farms.
$w \in W_i$	Set of wind farms connected to bus i .
$i \in B_w$	Set of buses connected to wind farm w .

B. Decision Variables

$n_{w,t}$ Binary variable equal to 0/1 if wind farm w is off/on at time t .

$P_{w,t}$ Wind farm's scheduled real power at time t .

$Q_{w,t}$ Wind farm's scheduled reactive power at time t .

C. Parameters

$P_{w,t}^{fore}$ Wind farm's forecasted real power at time t .

$Q_{w,t}^{fore}$ Wind farm's forecasted reactive power at time t .

Nomenclature 3: Chapter 5

A. Sets

$h \in H$ Set of PSH units.

$h \in H_i$ Set of PSH units connected to bus i .

$i \in B_h$ Set of buses connected to PSH unit h .

B. Decision Variables

$n_{h,t}$ Binary variable equal to 0/1 if PSH unit h is off/on at time t .

$S_{h,t}^g$ Binary variable represent PSH unit h is in generation mode at time t .

$S_{h,t}^p$ Binary variable represent PSH unit h is in pumping mode at time t .

$P_{h,t}$ Net output power of PSH unit h at time t .

$P_{h,t}^g$ Generation power of PSH unit h at time t .

$P_{h,t}^p$	Pumping power of PSH unit h at time t .
Vol_t	Volume of water stored in the reservoir at time t .
$q_{h,t}$	Net discharge rate of PSH unit h at time t .
$q_{h,t}^g$	Generation discharge of PSH unit h at time t .
$q_{h,t}^p$	Pumping discharge of PSH unit h at time t .

C. Parameters

$P_h^{g,\max}$	Maximum power limit of PSH unit h in generation mode.
$P_h^{g,\min}$	Minimum power limit of PSH unit h in generation mode.
$P_h^{p,\max}$	Maximum power limit of PSH unit h in pumping mode.
$P_h^{p,\min}$	Minimum power limit of PSH unit h in pumping mode.
Vol^{\max}	Maximum reservoir volume.
Vol^{\min}	Minimum reservoir volume.
q_h^{\max}	Maximum discharge rate of PSH unit h .
q_h^{\min}	Minimum discharge rate of PSH unit h .

Chapter 1: Introduction

1.1 Background

Recently, a number of high-impact low-probability (HILP) incidents have threatened the security of the bulk electric power system more frequently than ever before. Whenever and wherever such kind of incidents occur, there will be operation violations in the grid and possibly a large loss of load electricity supply in the power system, which can potentially lead to a system-wide blackout. The causes of electricity outages in power systems include earthquake/tsunamis, weather-related HILP events, cyber-attacks and operations error [1]. Based on the database from the U.S. Department of Energy (DOE), nearly 78% of the reported 1,333 electric grid disruptions in the period from 1992 to 2008 were weather-related (see Figure1) [2] - [5]. Similarly, there were a total of 178 weather-related blackouts in the United State alone, which reached or exceeded 1 trillion U.S. dollars damages or costs [6]. Because the bulk electric power system owns the control systems for generation and transmission, it relies on modern communication technologies to collect data and software implementations to make informed decisions, such as Supervisory Control and Data Acquisition Systems (SCADA), Large Power Plant Distributed Control Systems, and Smart Grid Technologies. With such communication platforms in place, the system has a higher vulnerability to be exposed to failures, delays, and cyber-attacks. For example, in 2015, a successful cyber-attack happened on the Ukrainian power system (among the first of its kind) leaving almost 225,000 people without power for approximately 6 hours [1].

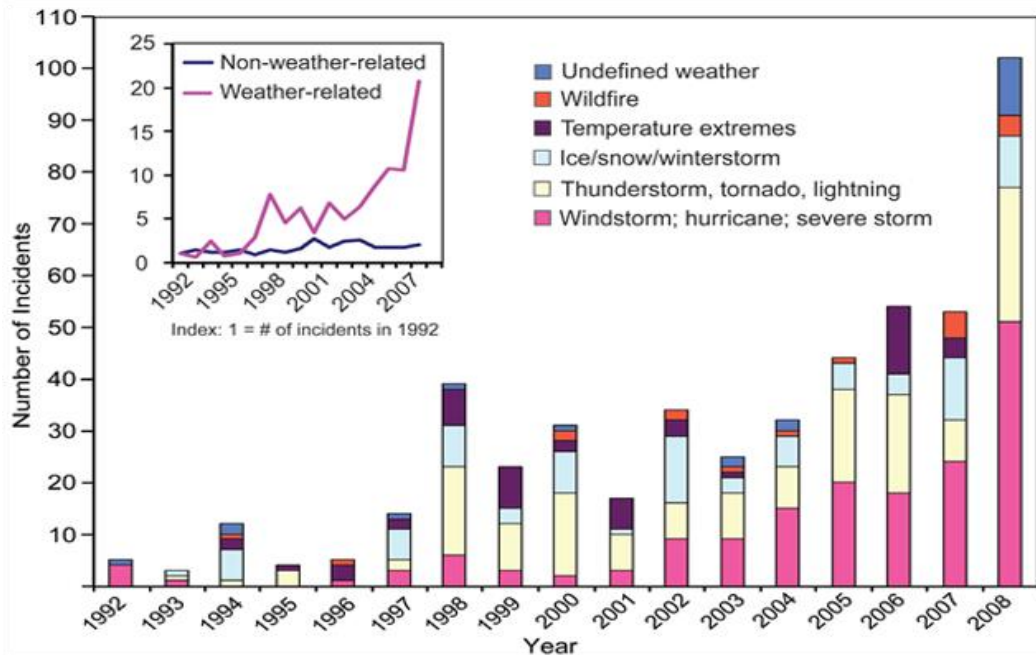


Figure 1 Significant weather-related U.S. electric grid disturbances [4].

When large-area blackouts occur, there are three consequences. Firstly, plenty of industries and companies are forced to suspend production for hours or days leading to significant economic loss. Secondly, these outages also cause water outages for dozens of people due to the loss of the electricity supply for normal operation of the water system. Note that the water distribution systems and power distribution systems are closely interdependent. Thirdly, those in need of specific health care at homes or hospitals would suffer health problem or even lose their lives because of the unserved electricity that was essential for their wellbeing [6] - [9]. Such long-duration damages, if not properly and swiftly recovered, will affect many sectors our lives depend on and all aspects of our economy [10] - [14]. Damages or costs of blackouts would actually be more severe, because the bulk electric system could not recover soon or spend several days on restoration. For instance, the 2003 blackout in North America left more than 50 million people without power up to 2 days, and estimated \$4 to \$10 million costs and 11 deaths

were reported. In certain outage areas, power was not restored even for 4 days [1] [15]. Similarly, during Hurricane Sandy striking the Eastern United States in 2012, 10 days of blackout in New York and New Jersey resulted in \$26 million costs and 50 deaths due to lack of electricity [1].

“Power delivery systems have a lot of parts, wires, transformers, and other components all nicely tied together – which means there are a lot of things that can go wrong,” explains Clark Gellings of the nonprofit Electric Power Research Institute (EPRI). “Pieces break down, and people make errors. A system is designed to tolerate a certain amount of disruption, but past a certain point it’s simply gone too far, and it falls apart.” EPRI has estimated that “across all business sectors, the U.S. economy is losing between \$104 billion and \$164 billion a year to outages.” [16]. Therefore, it is quite important to design effective strategies for system restoration to decrease the recovery time, reduce the costs from electricity outages and more importantly enhanced resilience against the grid-scale blackouts [17] - [27].

1.2 General Review for Restoration

After a large-area, long-duration blackout occurs, electric power system operators need to take a series of activities to return systems online as soon as possible. The process of recovering a power system from blackout is defined as *restoration*. Generally, a successful restoration procedure usually requires electricity providers to evaluate the extent, locations and severity of damage to the power system, provide the physical and human resources for stratifying requirements for repairs, set priorities for recovery based on the criticality of the load and the availability of resources to complete the needed repairs, as

well as implement the required repairs and reevaluate system status [1]. In fact, these general restoration processes would be executed at different scales by different electricity organizations. In other words, different organizations have their own restoration strategies, for example PJM (see Figure 2) [28].

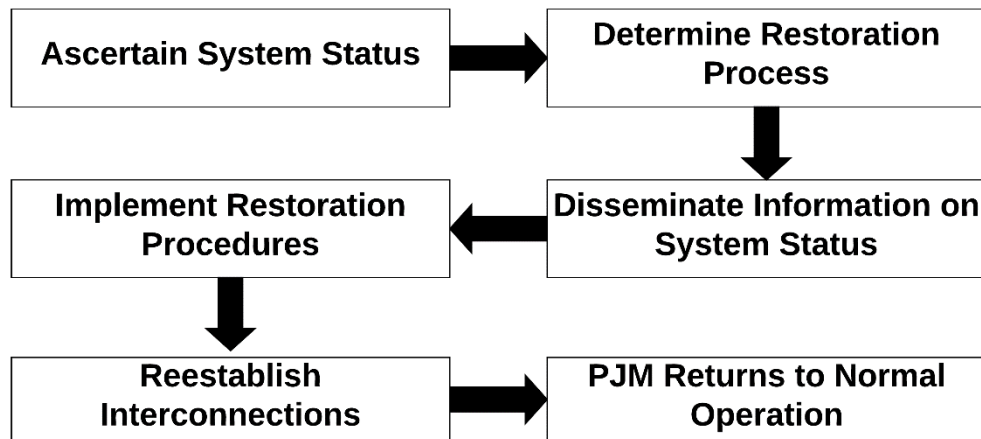


Figure 2 Restoration Process [28].

- *Ascertain System Status*: When a system blackout happens in a widespread area, it is important for system operators to find out the loss of generation and transmission, check equipment damage, and assess the extent of the service interruption. With the help of communications between the system operators as well as the Generation and Transmission Owners, operators can easily collect specific information after a system outage occurs. Utilizing the acquired information, PJM operators can determine the extent of outage, real-time generators status and transmission capabilities. Then, the system operators can move to the next step.
- *Determine Restoration Process*: After determining generators and transmission system status, system operators begin to design and develop a restoration strategy. In the process of designing a restoration plan, system operators need to apply

Energy Management System (EMS) to evaluate any actual overloads while recovering the system. Also, operators may need to utilize a manual monitoring procedure to assess dispatch factors of load outages at different nodes. Next, PJM operators need to apprise established restoration strategy to the Generation and Transmission Owners through communication systems.

- *Disseminate Information on System Status:* It is significant for system operators to provide updated information of the system status for all system restoration participants, because all participants need to execute the restoration strategy based on the real-time system conditions. In this step, PJM operators and Generation and Transmission Owners need to have closer cooperation and more frequent information exchange. For PJM operators, they would monitor generators and transmission system data for Generation and Transmission Owners, and coordinate the restoration strategy and system control for all participants. For Generation and Transmission Owners, they should update a real-time status of procedures for implementing the restoration plan to PJM operators.
- *Implement Restoration Procedure:* After PJM operators establish a restoration plan and disseminate information related to the generation and transmission availability, the system must restart internal generators and resupply demands while maintaining the system load, scheduled frequency, reasonable voltage level, and enough reserves. In this step, the restoration strategy works on the individual Transmission Owner that is in a total isolated or blackout condition and must restore its system without having any help from the outside/neighborhood systems. During the restoration procedure, operators need to control the system frequency which is

regulated between 59.75Hz and 61.0 Hz and maintain a suitable voltage level which is generally 90% to 105% of nominal.

- *Reestablish Interconnections:* When Transmission Owners accomplish the restoration process, they should make a preparation strategy and follow specific criteria to interconnect with other Transmission Owners. Before synchronization, each Transmission Owner must regulate the frequency of the lower level system to match the frequency of the higher level system. Similarly, operators of Transmission Owners not only control the voltages of interconnected areas as closely as possible, but also supply adequate reserves which are able to cover the largest energy contingency within the interconnected areas. While satisfying these conditions, interconnections of different Transmission Owners would be rebuilt.
- *PJM Returns to Normal Operation:* After restoration of individual Transmission Owner and reestablishment of interconnections, PJM operators would check permitted conditions for normal operation. When conditions permit, PJM operators identify all Generation/Transmission Owners returning to normal operation [28].

Similar to the PJM procedure, other electricity organizations such as the Cuivre River Electric Cooperative in Missouri (CREC), New York State Electric and Gas Corporation (NYSEG) and Rochester Gas and Electric Corporation (RGEC) possess their own restoration strategy following step by step procedures [1].

1.3 Research Motivation

Nowadays, large-scale electricity outages on power systems have become more commonplace as an alarming frequency and strength of natural disasters is reported more

frequently. In 2018, natural disasters which causes huge damages occurred every few weeks [29]. Hence, it is important to design and determine a more efficient and effective restoration strategy for a power system when a large-area, long-duration outage occurs. As mentioned in Section 1.2, several restoration processes should be executed sequentially in order to incrementally return the system back to its normal operating conditions. If power system operators could reduce the restoration time or decrease the economic losses at any step of the restoration procedure, an enhanced resilience would be then achieved in the face of such emergencies. For example, with an optimal generator start-up sequence or a transmission recovery path, electricity demands would be supplied faster at an *implemented restoration procedure*.

As deployment of wind energy is rapidly increasing worldwide, system operators should consider the influence and contributions of wind power while designing the restoration strategies. The record published in 2015 claimed that more than 63 GW of new wind power was brought on line globally [30]. In 2008, DOE published a report that set a goal of achieving 20% wind energy supply of the country's electricity by 2030 [31] [32]. In 2018, wind power generated 6.5% of the nation's electricity and even delivered over 20% of the electricity produced in six states [33]. Because the wind power plays increasingly important role in today's and tomorrow's electric power systems, many researchers discuss about incorporating wind power in power system operation, such as unit commitment and economic dispatch [34] [35]. For power system restoration planning, it is also necessary to incorporate wind energy and its contributions into the problem [36].

With the rapid developments of the energy storage solutions, the application of energy storage systems (ESS) for restoration planning has been discussed frequently, such

as participation of plug-in hybrid electric vehicles (PHEVs) in the recovery process and scheduling of mobile power sources (MPS) for resilience enhancement [37] - [40]. However, PHEVs and MPS only have a positive impact on distribution system restoration, and they currently do not have the ability to supply enough energy to reach the needs of the bulk transmission system restoration. In transmission systems, pumped-storage hydro (PSH), a type of hydroelectric energy storage, can satisfy the requirement of the energy supply for system operation and restoration during and following the emergencies, thereby enhancing the system resilience. Therefore, the objective of this thesis is to design an advanced restoration strategy that coordinates the operation of wind energy with PSH.

1.4 Thesis Outline

In this thesis, an advanced system restoration strategy for a power system following a blackout is proposed. There are three steps to develop such an advanced restoration strategy. Firstly, an optimal recovery path for the transmission system in a base-case system configuration without wind farms and PSH units is developed. Secondly, incorporating wind farms into the proposed restoration process, the efficiency and effectiveness of the restoration strategy in different scenarios are studied and extensively analyzed. Finally, we discuss the influence of PSH integrated in the restoration process for a transmission system test case with wind farms. The developed restoration strategy is tested on the IEEE 57-bus test system with numerical results that justify and verify the roles of wind energy and PSH units for restoration and recovery.

The remainder of this thesis is organized as follows. **Chapter 2** reviews the past work and literature on the applications of different methods and techniques for the system

restoration and enhanced resilience. It also provides a brief review of several research efforts on considering the impact of renewable sources on the system restoration.

Chapter 3 develops an optimization model for power grid restoration following an emergency. Several binary variables are introduced to represent a start-up sequence for generating units and an energization sequence for transmission buses and transmission lines. A mixed-integer linear programming (MILP) optimization model is utilized and solved in the GAMS optimization platform. The optimal generator start-up and transmission recovery sequence is achieved and the total load pickup curve during the restoration period is then presented.

Chapter 4 discusses the impact and contribution of the wind energy in the system restoration. A wind farm is installed in the test system. Through integration of the wind farm characteristics into the optimization model, simulation of the restoration process with the addition of wind energy is proposed. The simulation results show that the wind farm setting in the system can increase the restoration capability significantly. Afterwards, the sensitivity analysis is demonstrated in this chapter. The analysis involves discussing the impact of wind energy penetration, studying the impact of the wind farm's location, and describing the impact of the number of wind farms deployed in the grid.

Chapter 5 presents the contribution of the PSH units to the system restoration. A model similar to that in previous chapters is established to demonstrate the system restoration efficiency when wind energy and the PSH operation is coordinated. There are three case studies proposed in this chapter, where the simulation results demonstrate that the PSH unit not only can reduce the restoration time and enhance the system resilience

to HILP events, but also decrease the amount of wind curtailment to achieve a maximum wind power utilization.

Chapter 6 finally provides the research conclusions and lays out the future research directions.

Chapter 2: Literature Review

2.1 Introduction

The black-start (BS) recovery plan is a common approach to recover the power system from a large-area, long-duration outage. A BS is the process of restoring a part of or the entire electrical grid to operation without relying on the energy from external electric power transmission networks [41] [42]. To develop an optimal BS recovery plan, there is extensive research and literature that have discussed several restoration methods based on the deployment and operation of BS units. In addition, as renewable resources increase their penetration in power systems, several research papers discussed the application of such resources during the system restoration process. In this chapter, we will introduce such restoration tools and mechanisms as well as the techniques that have been explored so far in the literature.

2.2 Application of the Black-Start Generating Units for Restoration

Most generators in the system require enough electricity for operation, so if these generators have gone offline, they must rely on energy from external electric power networks to return back to the normal operation [1]. These kinds of generators are called non-black-start (NBS) generating units. On the contrary, there are BS generators that do not require power from the external grid to function. When BS generators operate normally, they can supply power to a system and provide cranking power for NBS generators: the power that NBS need to start a successful operation. The restoration process with black-start generators is called BS recovery plan. In fact, a BS recovery plan is difficult to practice

and implement, because of the complexity and nonlinearity in the system topology. When designing a BS recovery plan, operators have to identify priority loads and restoration of other NBS generation plants and emergency demands such as hospital services and military usages to determine an optimal recovery path, from high to low priority loads.

During the restoration process, the operators need to take a series of activities including evaluating system conditions, starting BS generating units, establishing transmission paths to supply cranking power to NBS generating units, picking up necessary loads to stabilize the power system, and synchronizing electrical islands [43] [44]. The revised standards EOP-005-2 [45] and EOP-006-2 [46] proposed a new definition of BS resources and requirements for Transmission Operators (TOP), Generator Operator (GOP) and Reliability Coordinators (RC). These two standards require each TOP to have a restoration plan approved by its RC, and each GOP to have a BS procedure which can satisfy BS testing requirements of its TOP [47]. Therefore, it is important for operators to utilize the available BS capabilities during the restoration process. Maximizing generation capability for restoration is a promising way to employ available BS generating units for providing cranking power to NBS generating units.

Generally speaking, the restoration process can be divided into three steps: starting generators, establishing transmission networks, and recovering load services [44]. In [48], authors provided a new algorithm to determine an optimal generator start-up sequence for BS restoration through global optimization process. The objective function of the proposed formulation is to maximize the generation capacity, and the constraints of the optimization model include binary variables to represent the status of generators. They developed a mixed-integer linear programming (MILP) model to solve the optimization problem and

achieve an optimal generator start-up sequence. After determining the generator start-up sequence, it is critical to find the shortest transmission recovery path. The paper [49] applies a similar MILP-based algorithm to determine an optimal transmission recovery path. With an optimal generator start-up sequence and the shortest transmission recovery path, it is important to design a proper method to resupply the load services. However, recovering load services is not as simple as the former steps.

Regulatory challenge is one of the restoration obstacles which are divided into three areas: regulatory, economic and technical challenges. Regulatory issues are associated with directives from the authorities in charge of determining the required level of service reliability to be supplied by utilities to the end users and customers [50]. Thus, many regulatory authorities, independent system operators (ISOs) and regional transmission organizations have proposed guidelines to ensure the service reliability during the restoration process [28] [45] [51] [52]. In [53], the authors describe that the ISO New England has addressed the system restoration regulatory, economic, and technical issues. They have also updated the change in restoration philosophy from a bottom-up to a top-down restoration plan.

The contributions in [53] inspired the authors in [54] and [55]. In [54], they concluded that it is critical to coordinate the generation and load pickup to ensure reliability during the load restoration process. This paper formulated a mixed-integer nonlinear load restoration (MINLR) model to determine a multi-stage decision process for load restoration. The simulation of the MINLR model is based on the BS restoration plan. Different from the algorithms in [48] and [49], the objective function of the suggested MINLR model is to maximize the load pickup subject to AC power flow and reserve constraints. Thus, this

methodology can assist the system operators to restore load services to the customers and conduct frequency/voltage control. Reference [55] proposes a decision support methodology for restoration of interconnected power systems through the application of tie lines (TLs). In this paper, authors formulated an optimization model to determine the optimal application of TLs and dispatch of available BS capabilities to NBS units.

There is also further literature discussing the BS recovery strategy from different aspects. Reference [56] introduces a new method that can optimize the generator start-up sequence and the associated restoration paths simultaneously. In this paper, authors formulated a multi-objective optimization model with three optimization objectives which are to maximize the generation capacity, the reliability of restoration paths, and the importance of restoration paths. In [57], authors proposed the application of Voltage Source Converter – High Voltage Direct Current (VSC-HVDC) for BS scheme to avoid the inrush current and transient over voltage. As for [58], it presents two indices of capacity selection for BS generating units and builds the MATLAB/SIMULINK model for implementing the presented indexes.

2.3 The Application of Renewable Resources for Restoration

With the increasing penetration of variable renewable energy resources, changes in system restoration strategies would be required. Different from the traditional generation resources which process a relatively predictable operating performance, renewable energy resources are attributed more variability and uncertainty, which at times, may challenge the grid operation and control [19]. For example, forecasts of wind may not be always accurate and the wind power output of a wind farm might rapidly change from 0% to 100%

of the rated capacity of the wind farm. Such uncertainties bring new challenge to the system restoration. However, renewable energy resources can bring several benefits to system restoration [16]. The first benefit of deploying renewable resources in the restoration process is to increase the BS capacity. When the frequency deviation reaches the threshold values of the protection requirements for generation units, they are automatically disconnected from the grid. Thanks to the Smart Grid Technologies, renewable resources may be permitted to contribute to BS, because the disconnection of wind generation units connected to the distribution system is often less strict than for units connected to the transmission grid [16] [59]. The second benefit is to ameliorate the load pickup conditions during restoration. Renewable resources could provide power to restore loads, when they satisfy all general requirements.

Reference [60] presents several aspects of power system restoration considering wind farms. The first aspect is the development of wind power technology. There are several technologies for wind generation that make a smooth wind control possible. These technologies involve a doubly fed induction generator (DFIG) based wind turbine and a permanent-magnet synchronous generator (PMSG) based wind turbine [61] - [64]. The second one is the target and constraints of wind farm restoration. The target of a wind farm is to determine whether to restore wind farms based on the amount of forecasted power, while the constraints of wind farms are to restrict the output power of the wind farms. This satisfies the power balance requirements. The third one is the influence on load restoration. Wind farms have a negative impact on load restoration, because of the DFIG characteristics which control the active power and reactive power independently [60].

In [63], authors developed a control system for the BS process with DFIG-based wind turbines. According to the simulations, it was concluded that the control system with DFIG can provide a strong capability for fast restoration of a network from BS. Similarly, reference [64] also designed a frequency control strategy for wind power generation (WPG) in the BS procedure (see Figure 3). The strategy in this paper is based on the PMSG-based wind turbines, where the authors presented that the application of PMSG-based WPG in the BS procedure can significantly enhance the resilience of the power systems.

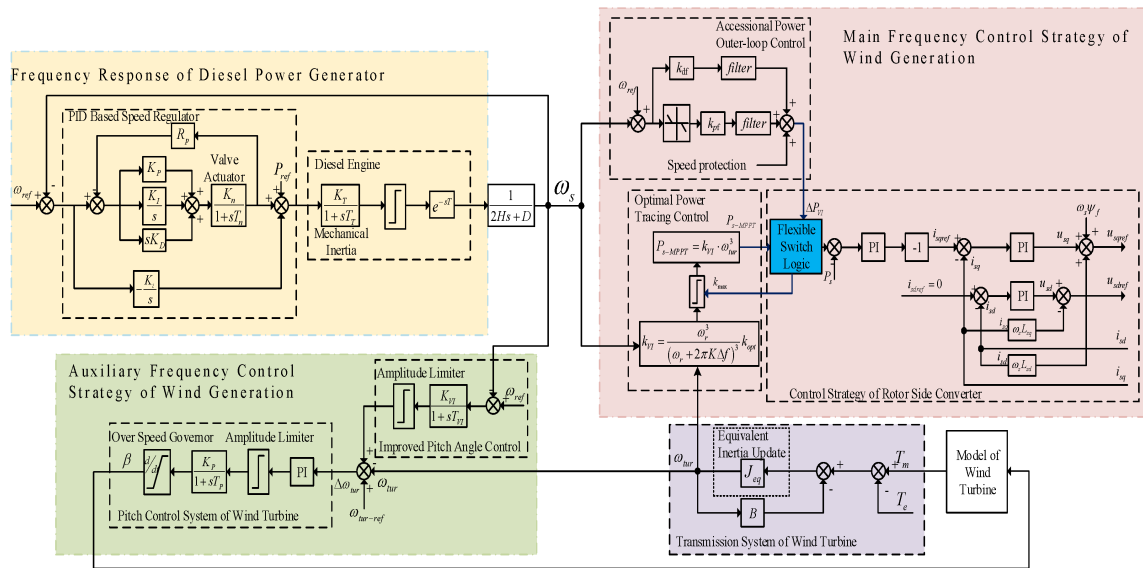


Figure 3 Coordinated frequency control for WPG participation in the BS procedure [64]

The flexibility offered by large offshore wind farms with VSC-HVDC technology is utilized to support the restoration following a blackout in a typical transmission grid [65]. The simulation results in [65] show that after the energization of the offshore wind farm, the load pick up in the system is faster than in the scenarios where no wind farm exists. Thus, authors concluded that the conventional synchronous generating units would be

replaced by the large-scale integration of renewable generation, which could be ready to run in a short time to fully support the restoration phase. In [66], the authors proposed the utilization of a firefly algorithm to find the optimal restoration strategy with the help of renewable energy resources.

Apart from the wind power, photovoltaic (PV) power is another resource of renewable energy. There are some research efforts on the effective utilization of the PV power in BS restoration. For example, reference [67] presents a BS scheme optimization model to maximize the total power provided by PV stations and energy storage units. The simulation results revealed that the full use of PV power and energy storage can recover as much traditional units and load as possible. Moreover, an allocation (sizing and siting) scheme is proposed in [20] that best allocates the PV and energy storage resources in transmission systems for maximum load pickup during emergencies, swift restoration and recovery following the HILP events, and an enhanced network resilience.

2.4 Other Techniques for Restoration

2.4.1 Topology Control for Restoration

Power system topology control, often called transmission line switching (TLS), can change the way how electricity flows through the system, so it provides operators an opportunity to utilize the flexibility of the transmission system topology [6]. Through temporarily removing transmission lines out from service, TLS can be applied not only in normal operating conditions for economic gains and financial benefits, but also during the system restoration for enhanced reliability and resilience [68] - [72]. Here, we only introduce the research on the application of TLS for system restoration.

When employing TLS for restoration, most previous studies developed the topology control optimizations. There is a review of past research on the applications of topology control optimization presented in [73]. In [74], authors proposed an optimal topology control with AC power flow constraints to decrease the system operating cost during N-1 contingency. A DCOPF-based TLS model is implemented to recover the load outages in case of critical contingencies in [75]. The authors in [76] presented a flexible decision making support tool based on the DCOPF model for TLS that ensures a reliable implementation of TLS solutions, mostly for load outage recovery. When implementing TLS in practice, operators would face three important issues, including circuit breaker monitoring, relay setting coordination, and detection of relay miss-operations [77]. The framework presented in this paper can satisfy the AC feasibility, stability, and circuit breaker reliability requirements needed for practical implementation. Reference [77] utilized an adaptive topology control to address these three issues.

2.4.2 Energy Storage for Restoration

There are also a large number of research efforts discussing about the application of energy storage for restoration. Reference [37] presented a new healer reinforcement approach to enhance the self-healing capability of the smart grids. The approach introduces plug-in hybrid electric vehicles (PHEVs) as backup sources and storage units in the restoration process. The presented results in this paper showed that with the help of PHEVs, the system operators can reduce the total cost of reliability and system average interruption duration indices. Similarly, the authors in [38] also utilized the PHEVs for restoration. They proposed a nonhomogeneous Markov chain method for generation of synthetic

driving behavior of PHEV owners. A new and completely distributed algorithm for restoration with distributed energy storage is presented in [39], where following extensive simulations of the presented algorithm, it was concluded that the distributed energy storage have several benefits to support the distribution network restoration. Mobile power resources (MPSs) are introduced to improve the restoration capacities of power distribution systems [40]. With a two-stage robust optimization model, the paper shows that the MPSs can reduce restoration time and enhance the system resilience.

The energy storage techniques mentioned above all work at the distribution level. At the transmission level, a complete dynamic model of the BS capable pumped-storage units is presented in [78].

2.4.3 Other Paradigms for Recovery and Resilience

In addition to the aforementioned techniques for restoration, there exist in the literature a wide-range of other approaches and considerations that individually or collectively help an improved system performance under normal operating conditions (enhanced situational awareness) and for resilience during emergencies. Such considerations range from the formation, deployment, operation and control of microgrids in distribution systems [79] - [81], advanced preventive and corrective maintenance strategies in generation, transmission and distribution systems [82] - [103], distributed generations (DGs) and remote-terminal units (RTUs) [104] - [112], advanced control and operation of EVs [113] - [119], and harnessing the data analytics on sensors and phasor measurements [120] - [127], among others.

Chapter 3: Formulations for System Restoration under the Base Case Scenario

3.1 Introduction

Utilizing black-start (BS) generating units to resupply electricity services from a huge blackout is a common and reliable approach for system restoration. Especially, BS generating units are indispensable parts of the self-healing smart power grids. The restoration strategy in this chapter is based on the utilization of BS generating units.

In this chapter, an optimization model for enhanced system restoration is developed and solved in a mixed-integer linear programming (MILP) model. According to the presented restoration strategy, an optimal generators start-up sequence and the shortest transmission recovery path would be achieved. The simulation result also would show the total load pickup during the restoration process. The case studies presented in this chapter are focused on the IEEE 57-bus test system.

3.2 Problem Formulation

The procedure of BS restoration in a transmission system includes the following four steps (see Figure 4):

- BS generating units begin to operate and produce the electric power.
- Transmission network is energized by BS generating units and recovered based on its topology.

- Non-black-start (NBS) generating units obtain cranking power through transmission lines from BS generating units and supply the electric power to transmission network when they are back to the normal operation.
- Electricity services for demands are supplied by the power transferred through transmission network.

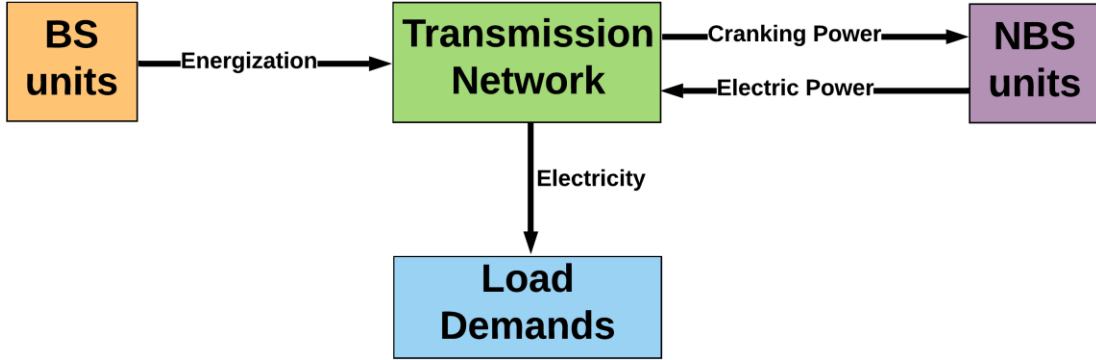


Figure 4 BS Restoration Process

An optimization model will be developed to simulate the BS restoration process. With the review of the past literature on the role of the BS generating units in the restoration process [47], system operators can optimize the use of available capacities in BS generating units by maximizing the total generation capability. Apart from maximizing the available BS capacities, increasing the load pickup at each time step during the restoration period should be also concerned. Thus, the objective function in the model is to maximize the total generation capability and minimize unserved load during restoration, as formulated below:

$$\max \left(\sum_{t \in T} \sum_{g \in G} (P_g^{\max} - P_g^{\text{start}}) n_{g,t} - \sum_{t \in T} \sum_{d \in D} \hat{\sigma}_d (P_d^{\max} - P_{d,t}) \right) \quad (3.1)$$

Where, binary variable $n_{g,t}^{on}$ represents the status of generating unit g at restoration time t , and decision variable $P_{d,t}$ represents the amount of restored load d at restoration time t . Parameters P_g^{\max} and P_g^{start} denote the maximum generation capacity and the amount of required cranking power for the generating unit g . P_d^{\max} is the maximum amount of restorable demand load d and ∂_d is the load priority factor of load d . Here, we use 10 minutes to denote one time step during the restoration process. To represent the restoration process, multiple constraints should be considered. The optimization constraints involve the initial conditions constraints, energization sequence constraints, components characteristics constraints, power balance constraints, and load pickup constraints.

3.2.1 Initial Conditions Constraints

In this thesis, it is assumed that the transmission system suffers a blackout because of the disturbance from other transmission systems which are affected by a large natural disaster (i.e., HILP events). Based on this assumption, there are no physical damages to the system components and major infrastructure, but the system suffers from an electricity blackout. All generating units readily participate in the restoration process. At the beginning of the restoration, none of the components in the system are energized. Constraints (3.2)-(3.5) imply that all generating units are off, and transmission buses and lines are de-energized at the initial time. Constraint (3.6) illustrates that the BS generating units begin to start operation at the first time step.

$$n_{g,t=0}^{start} = 0, \quad g \in G \quad (3.2)$$

$$n_{g,t=0} = 0, \quad g \in G \quad (3.3)$$

$$n_{i(j),t=0} = 0, i \in B \quad (3.4)$$

$$n_{k,t=0} = 0, k \in K \quad (3.5)$$

$$n_{g,t=1}^{start} = 1, g \in G_{BS} \quad (3.6)$$

Where, binary variables $n_{g,t}$, $n_{i(j),t}$ and $n_{k,t}$ represent the status of generating unit g , bus i and transmission line k . When these binary variables are equal to 1, then the generating unit g is online, bus i and transmission line k are energized. Binary variable $n_{g,t}^{start}$ denotes whether the generating unit g is in the start-up period. If generating unit g is in start-up period, it is equal to 1.

3.2.2 Energization Sequence Constraints

During the system restoration, the recovery path of transmission network should obey a logical energization sequence (see Figure 5), which requires transmission buses and lines being re-energized one by one. This is enforced by the energization constraints.

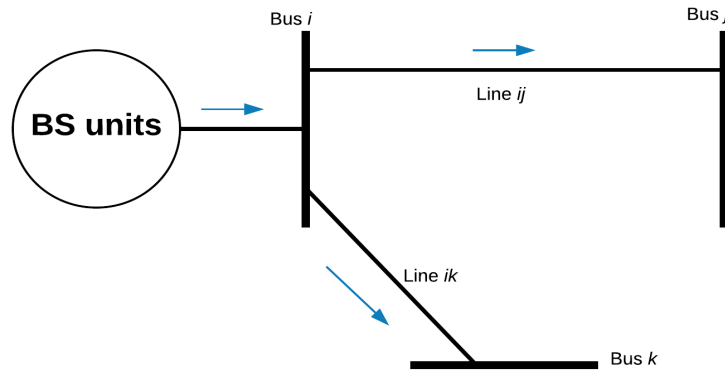


Figure 5 Illustration of logical sequences for transmission path

Energization sequence constraints can be divided into two parts: generating units' start-up and transmission buses/lines re-energization. In the generation units' start-up part, BS generating units have different start-up sequences with NBS generating units. As for the BS generating units, when they operate normally, the buses connected to them would be energized, which is represented in constraints (3.7). Because NBS generating units require cranking power from an outside network, the NBS can start only after the buses connected to them receive the electric power in (3.8).

$$n_{g,t} \geq n_{i,t}, \quad g \in G_{BS}, i \in B_{BS} \quad (3.7)$$

$$n_{g,t}^{start} \leq n_{i,t}, \quad g \in G_{NBS}, i \in B_{NBS} \quad (3.8)$$

For all off-line generation units, they need to spend time on returning back to a normal operation after the required cranking power is delivered. The consumed time in the start-up period is determined depending on the type of the generators. Hydro generators can be started quickly without outside sources (i.e., BS unit), while combustion turbines (CT) would take 10 minutes to 1 hour in start-up period depending on their capacities. For steam turbines, they typically spend 1 to 20 hours on start-up relying on their status. Constraint (3.9) denotes that generating unit g is on line after the start-up period, and T_s represents the start-up duration of generating unit g .

$$n_{g,t+T_s} \leq n_{g,t}^{start}, \quad g \in G \quad (3.9)$$

In transmission buses/lines re-energization part, they also need to follow a logical transmission path. If connected buses are de-energized at time t , the transmission line is also de-energized at time t . In other words, a transmission line is energized, only when any buses connected to it is energized. Constraint (3.10) denotes this relationship. After a bus is energized, it will take one time step to energize the line connected to this bus. Constraint

(3.11) illustrates that if a line is energized at $t+1$, then at least one of the buses connected to it is energized at time t .

$$n_{k,t} \leq n_{i(j),t}, \quad i, j \in B_k \quad (3.10)$$

$$n_{k,t+1} \leq n_{i,t} + n_{j,t}, \quad i, j \in B_k \quad (3.11)$$

For a bus connected to the NBS generating units, if all transmission lines connected to this bus are de-energized at time t , this bus is also de-energized at time t . Constraint (3.12) shows that a bus connected to NBS generating unit is energized, when any transmission lines connected to this bus is energized.

$$n_{i,t} \leq \sum_{k \in K_i} n_{k,t}, \quad i \in B / B_{BS} \quad (3.12)$$

Constraints (3.13) and (3.14) present that once a bus or transmission line is energized, it won't be de-energized again.

$$n_{i,t} \leq n_{i,t+1} \quad (3.13)$$

$$n_{k,t} \leq n_{k,t+1} \quad (3.14)$$

3.2.3 Components Characteristics Constraints

In this section, constraints characterized by the component characteristics are taken into account which consist of generator parameters, generator start-up characteristics, transmission line characteristics and load characteristics. The output power of a generator should be limited by its real and reactive power capacity. Constraints (3.15) and (3.16) show the minimum and maximum boundary of the real and reactive power output of generating unit g . The output power of each generator is restricted by its ramping rate – the rate at which a generator can increase or decrease its output, as shown in constraint (3.17).

Similarly, constraints (3.18) and (3.19) illustrate the real and reactive power limitation of transmission lines, while constraints (3.20) and (3.21) present the capability of real and reactive loads.

$$P_g^{\min} n_{g,t} \leq P_{g,t} \leq P_g^{\max} n_{g,t} \quad (3.15)$$

$$Q_g^{\min} n_{g,t} \leq Q_{g,t} \leq Q_g^{\max} n_{g,t} \quad (3.16)$$

$$-RR_g \leq P_{g,t+1} - P_{g,t} \leq RR_g \quad (3.17)$$

$$P_k^{\min} n_{k,t} \leq P_{k,t} \leq P_k^{\max} n_{k,t} \quad (3.18)$$

$$Q_k^{\min} n_{k,t} \leq Q_{k,t} \leq Q_k^{\max} n_{k,t} \quad (3.19)$$

$$P_d^{\min} n_{i,t} \leq P_{d,t} \leq P_d^{\max} n_{i,t}, \quad i \in B_d \quad (3.20)$$

$$Q_d^{\min} n_{i,t} \leq Q_{d,t} \leq Q_d^{\max} n_{i,t}, \quad i \in B_d \quad (3.21)$$

The generator start-up characteristics illustrate the amount of energy consumption by the NBS generating units. During the start-up period, the NBS generating units require cranking power from external transmission systems. Constraint (3.22) represents the required cranking power for generating unit g at time t .

$$P_{g,t}^{start} = P_g^{start} (n_{g,t}^{start} - n_{g,t}), \quad g \in G_{BS} \quad (3.22)$$

3.2.4 Power balance constraints

Real and reactive power generation and load have to be balanced at all times in each bus, as shown in constraints (3.23) and (3.24). Constraints (3.25) and (3.26) represent the power flow balance at each transmission line.

$$\sum_{g \in G_i} (P_{g,t} - P_{g,t}^{start}) - \sum_{d \in D_i} P_{d,t} = \sum_{k \in K_f} P_{k,t} - \sum_{k \in K_t} P_{k,t} \quad (3.23)$$

$$\sum_{g \in G_i} Q_{g,t} - \sum_{d \in D_i} Q_{d,t} = \sum_{k \in K_j} Q_{k,t} - \sum_{k \in K_i} Q_{k,t} \quad (3.24)$$

$$P_{k,t} = V_{i,t} g_k - V_{i,t} V_{j,t} (g_k \cos \theta_{k,t} + b_k \sin \theta_{k,t}) \quad (3.25)$$

$$Q_{k,t} = -V_{i,t}^2 (b_k + b_{k0}) + V_{i,t} V_{j,t} (b_k \cos \theta_{k,t} - g_k \sin \theta_{k,t}) \quad (3.26)$$

However, AC power flow constraints (3.25) and (3.26) are nonlinear, so a linearized model for AC power flow is included in constraints (3.27) and (3.28). This approach is introduced in [128], and the details are presented in Appendix 1. Typically, the bus voltage magnitude has a range from 0.95 p.u. to 1.05 p.u. and absolute value of phase angle difference across transmission line k is lower or equal than 90° . Constraints (3.29) and (3.30) illustrate the boundary for the bus voltage magnitude and phase angle.

$$P_{k,t} = (\Delta V_{i,t} - \Delta V_{j,t}) g_k - b_k \theta_{k,t} \quad (3.27)$$

$$Q_{k,t} = -(1 + 2\Delta V_{i,t}) b_{k0} - (\Delta V_{i,t} - \Delta V_{j,t}) b_k - g_k \theta_{k,t} \quad (3.28)$$

$$-0.05 n_{i,t} \leq \Delta V_{i,t} \leq 0.05 n_{i,t} \quad (3.29)$$

$$-\frac{\pi}{2} n_{k,t} \leq \theta_{k,t} \leq \frac{\pi}{2} n_{k,t} \quad (3.30)$$

Where, $\Delta V_{i,t}$ denotes the voltage magnitude deviation from 1 p.u. at bus i , and $\theta_{k,t}$ represents phase angle difference across transmission line k . Parameters b_k and b_{k0} are series admittance of transmission line k and shunt admittance of transmission line k , while parameter g_k is the conductance of the transmission line k .

3.2.5 Load Pickup Constraints

During restoration, operators should consider the amount of dynamic reserve that is available in order to preserve the system during a frequency disturbance, which in turn, allows the system to survive the loss of the largest outages [28]. The required amount of dynamic reserve should be determined by “load pickup factors” which are the maximum amount of load a generator can pick up without resulting in a reduction of frequency below the prescribed safe operation level (57.5Hz). The values of load pickup factors are dependent on the type of generators. The factor is assumed to be 5% of the generation capacities in steam turbines, 15% of the generation capacities in hydro generators, and 25% of the generation capacities in combustion turbines. Constraint (3.31) presents the maximum load pickup capacity at each restoration time. Once the load buses are supplied by the required electricity, they would not lose their load again as enforced in (3.32).

$$\sum_{d \in D} P_{d,t+1} - \sum_{d \in D} P_{d,t} \leq \sum_{g \in G} \lambda_g P_{g,t} \quad (3.31)$$

$$P_{d,t+1} - P_{d,t} \geq 0 \quad (3.32)$$

3.3 Case Study

A modified IEEE 57-bus test system has been adopted in this chapter, the one-line diagram of which is illustrated in Figure 6. The system has 7 generators, and the total amount of load outage is 1250 MW. The data for the IEEE-57 bus system is provided in Appendix 2. The base power is assumed to be 100 MW and each restoration time step is 10 minutes (1 p.u.). The total restoration period is 5 hours (30 p.u.). The formulated MILP model is simulated in the GAMS optimization platform.

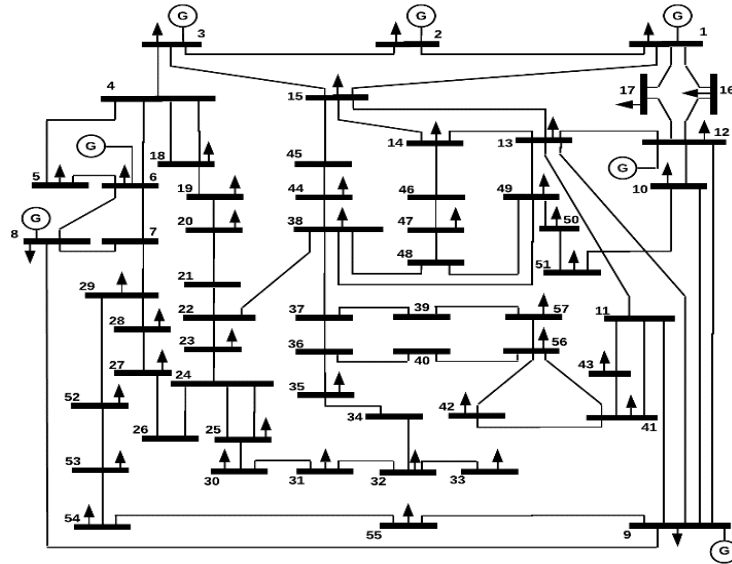


Figure 6 IEEE 57 Bus system

3.3.1 Optimal Generator Start-up Sequence

According to Table 1, all generators are operating normally (online) after 3 hours (18 p.u. time). The cranking power supply path corresponding to the generator 5 is the longest, as shown in Table 2.

Table 1 Optimal Start-up Time for Generators

Gen. No.	Time (p.u.)	Type	Gen. No.	Time (p.u.)	Type
G1	2	Hydro turbine	G5	18	Steam turbine
G2	9	Steam turbine	G6	8	Steam turbine
G3	10	Steam turbine	G7	16	Combustion turbine
G4	9	Combustion turbine			

Table 2 Cranking Power Supply Path

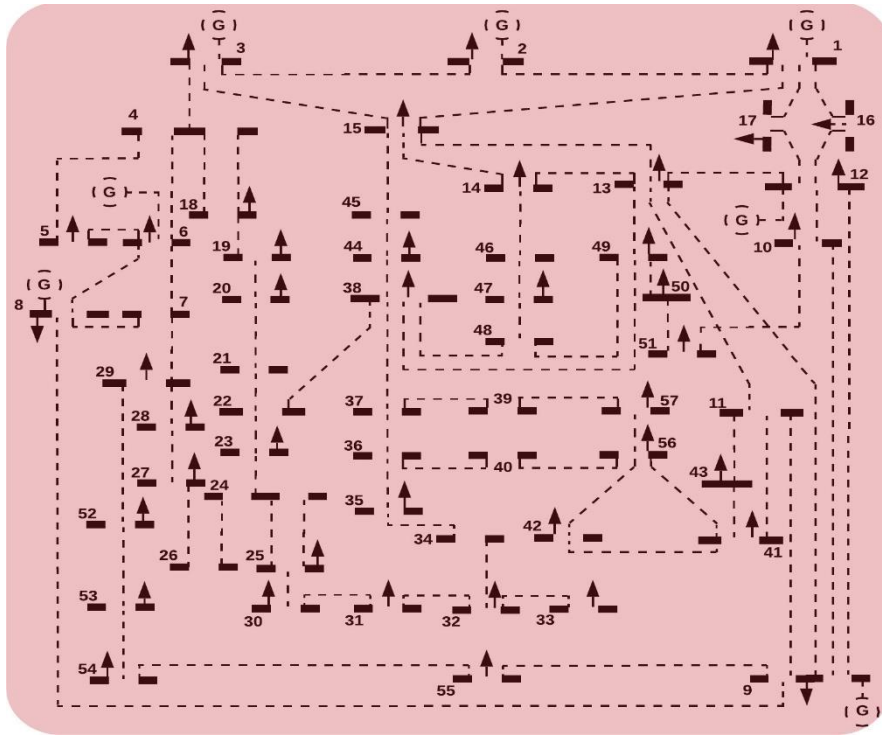
NBS gen.	Supply Path
G2	Bus: 1→2
G3	Bus: 1→2→3
G4	Bus: 1→2→3→4→6
G5	Bus: 1→15→13→9→8
G6	Bus: 1→15→13→9
G7	Bus: 1→16→12

3.3.2 Optimal Transmission Re-energization Path

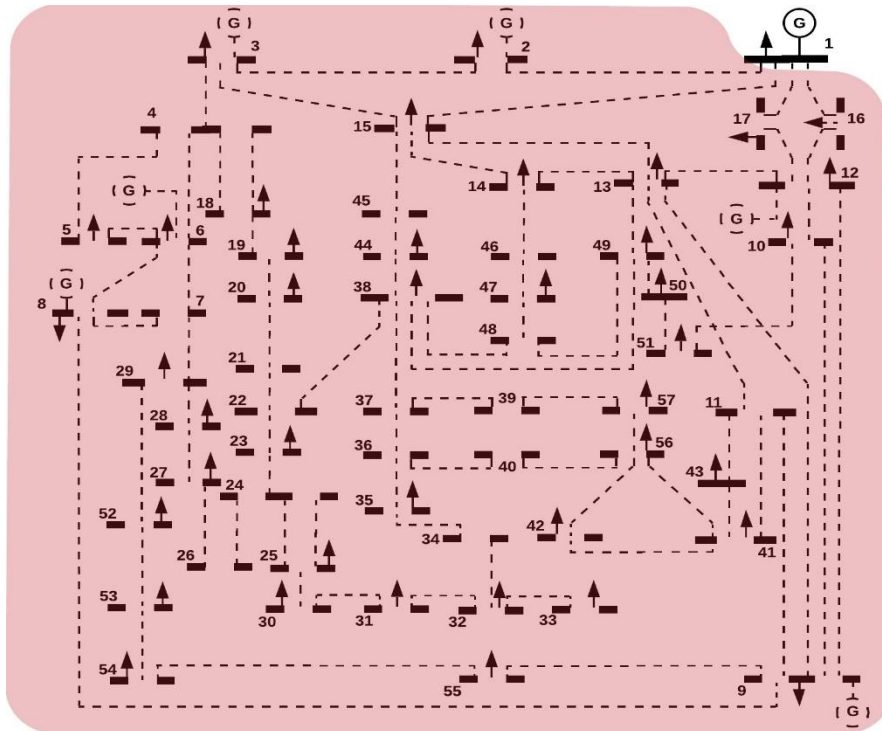
Figure 7 shows the restoration path for the IEEE 57-bus test system during each time interval. In this figure, the solid lines represent the transmission buses/lines that are energized, while the dashed lines denote the transmission buses/lines that are de-energized. Based on this figure, it takes 12 p.u. time (2 hours) to energize all transmission buses and lines. Although the studied transmission network can be recovered within 2 hours, the total demand loads need more time to restore. The reason lies in the fact that some NBS generating units spend more than 2 hours for start-up. Table 3 illustrates the amount of restored loads at each time interval during the transmission network recovery.

Table 3 The Amount of Demand Loads at Each Time Step

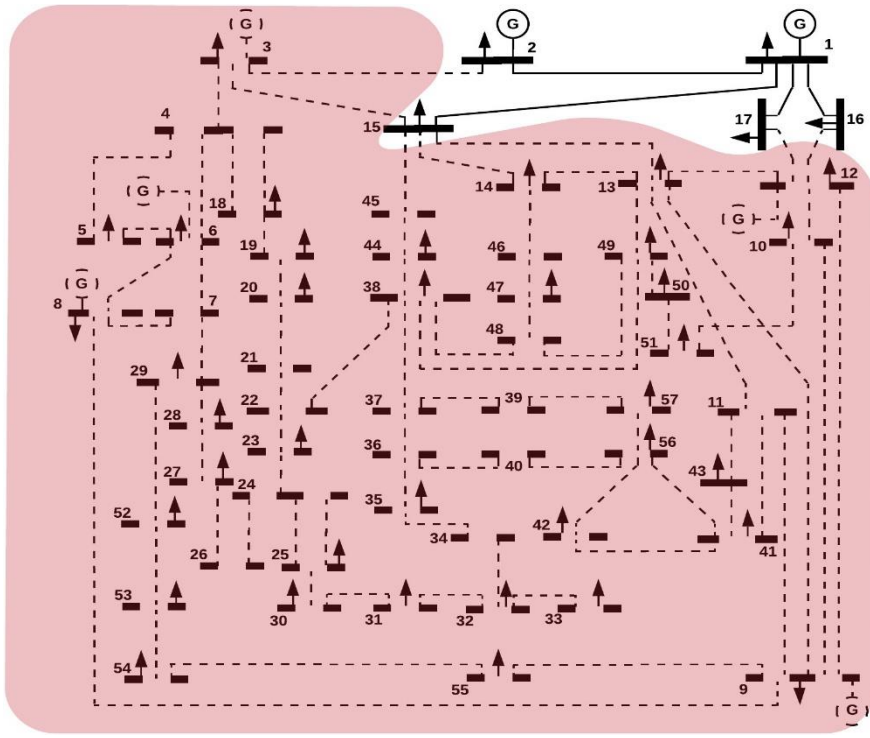
T (p.u.)	1	2	3	4	5	6
Total Demands (MW)	1250	1250	1250	1250	1250	1250
Restored Loads (MW)	0	50	99	137	181	217
Outages (MW)	1250	1200	1151	1113	1069	1033
T (p.u.)	7	8	9	10	11	12
Total Demands (MW)	1250	1250	1250	1250	1250	1250
Restored Loads (MW)	267	373	569	766	887	977
Outages (MW)	983	877	681	484	363	273



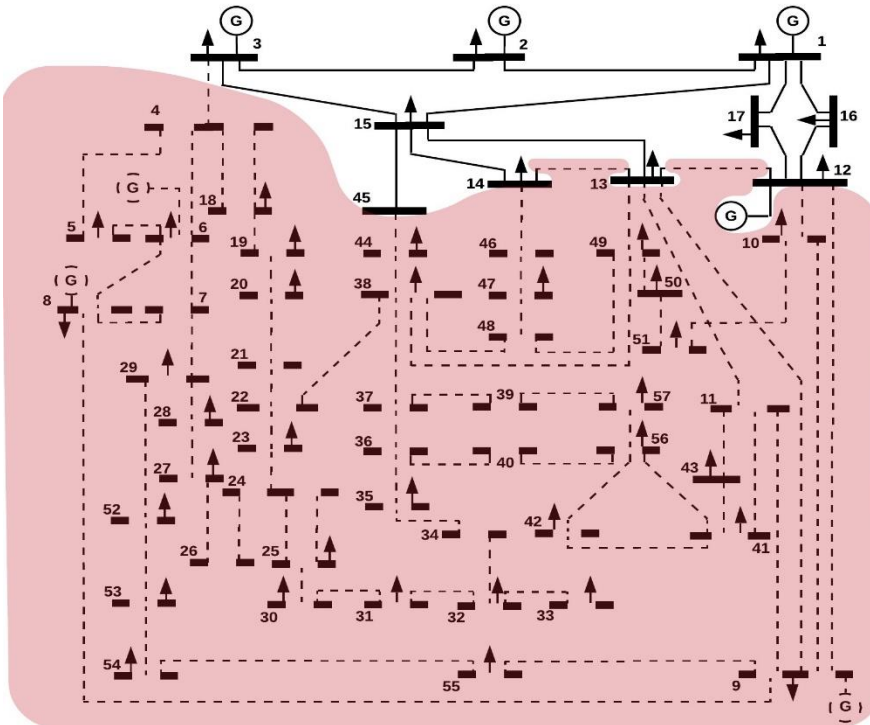
(a)



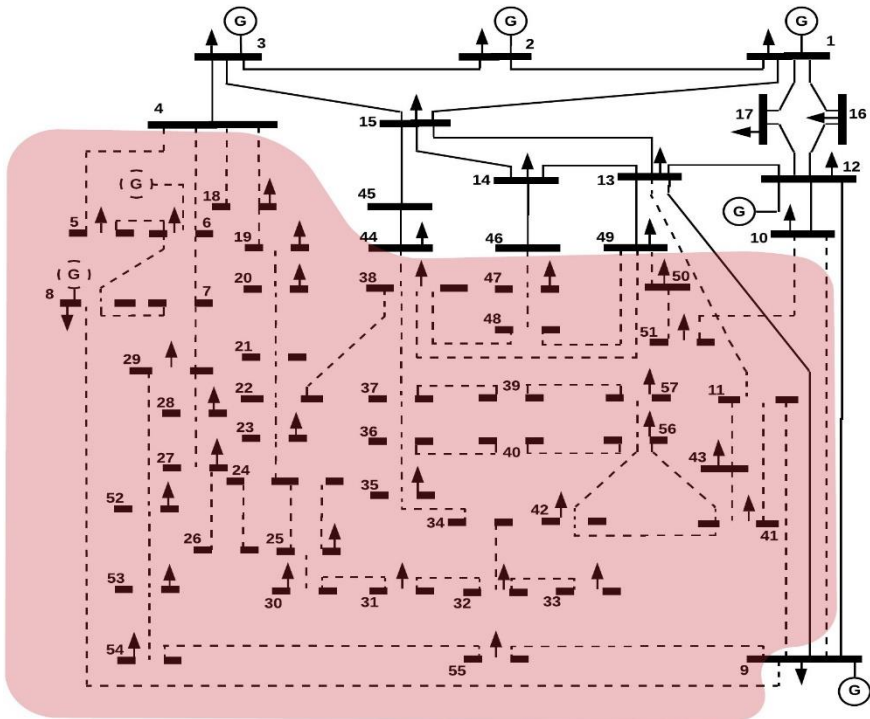
(b)



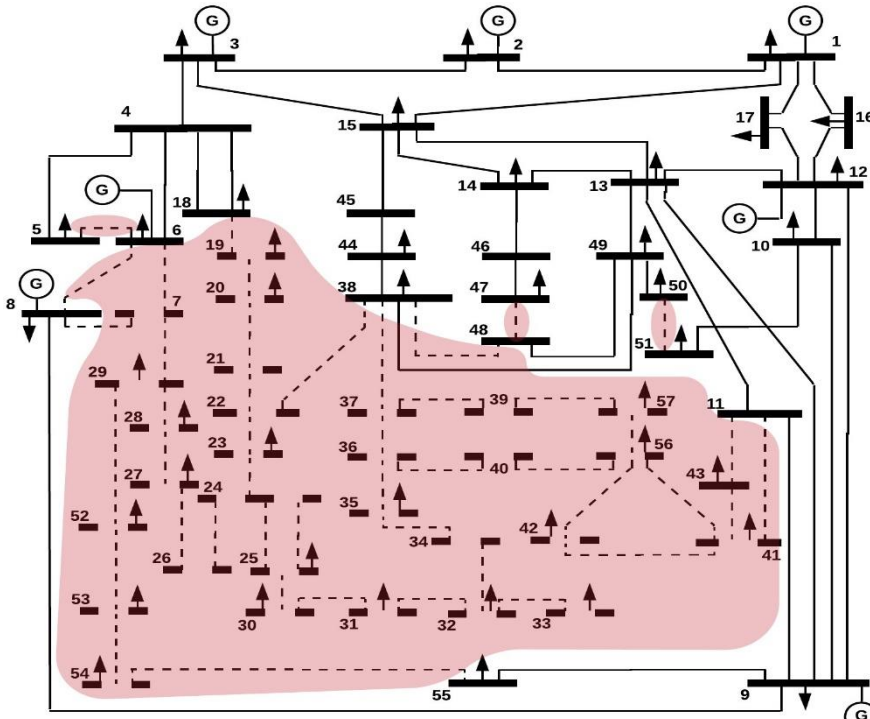
(c)



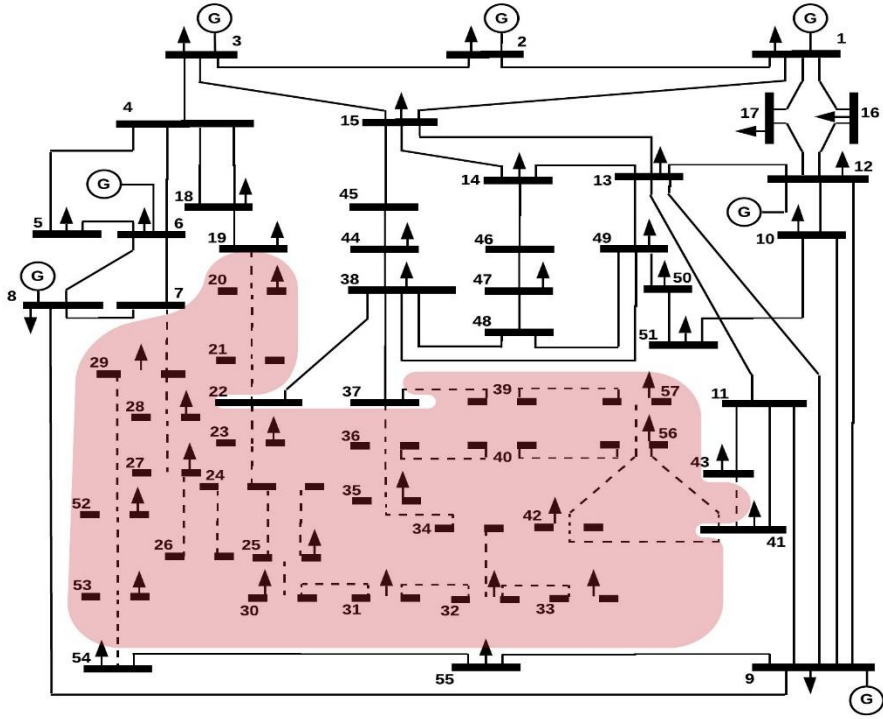
(d)



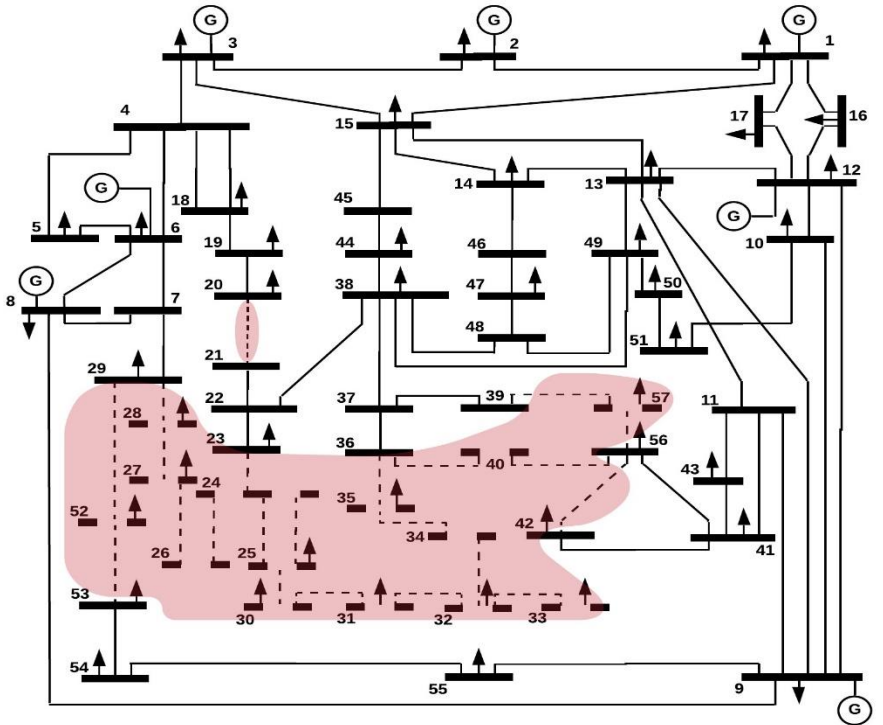
(e)



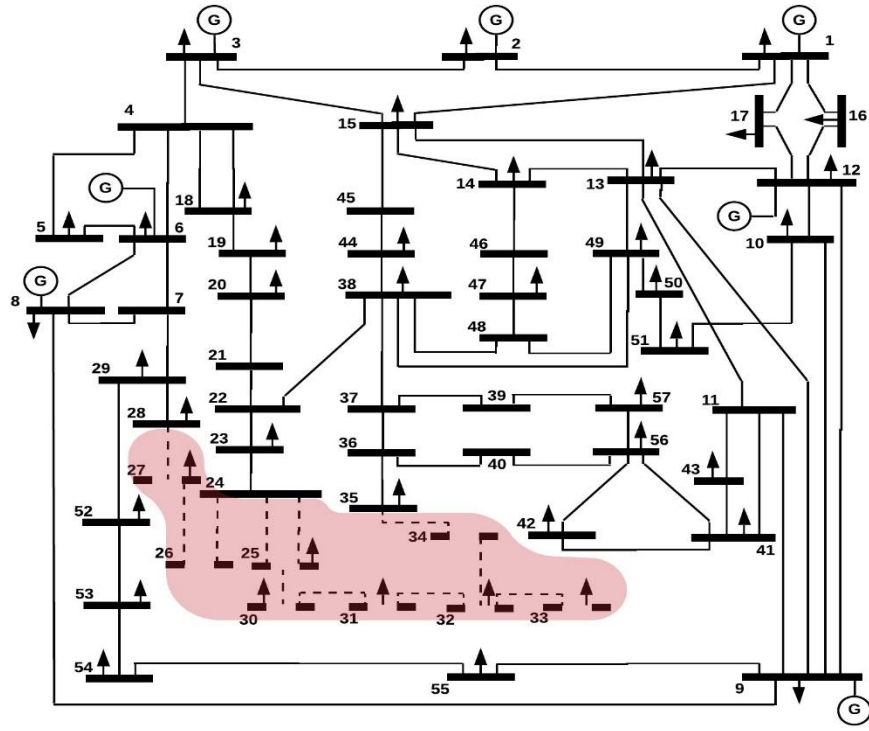
(f)



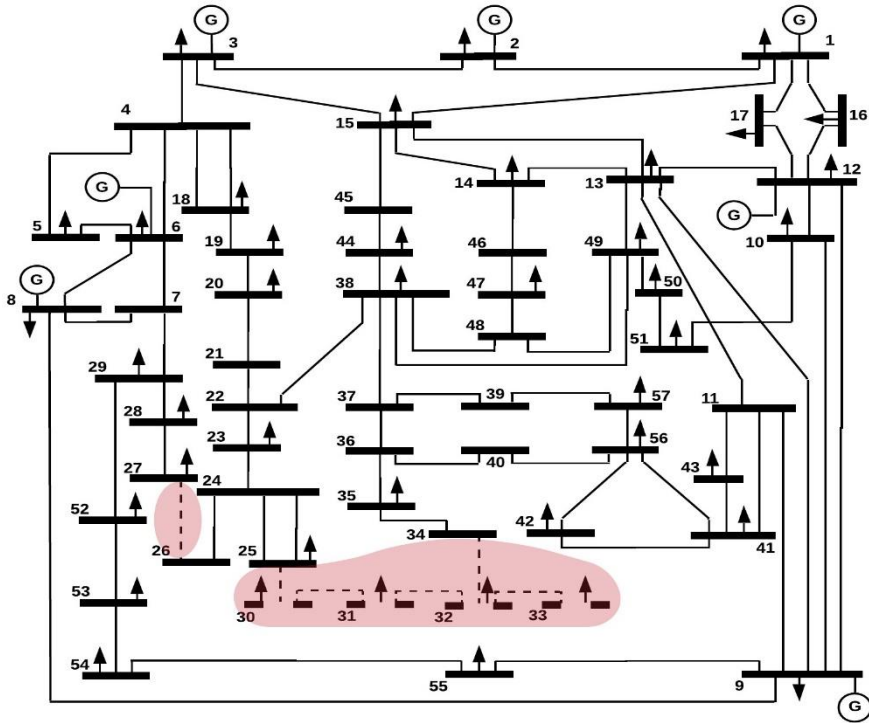
(g)



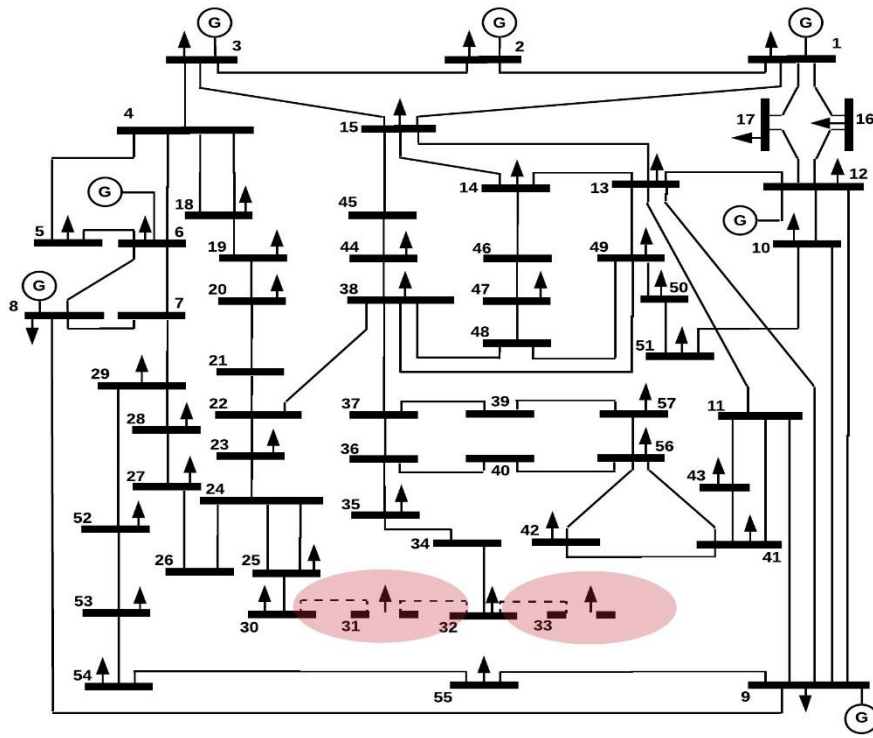
(h)



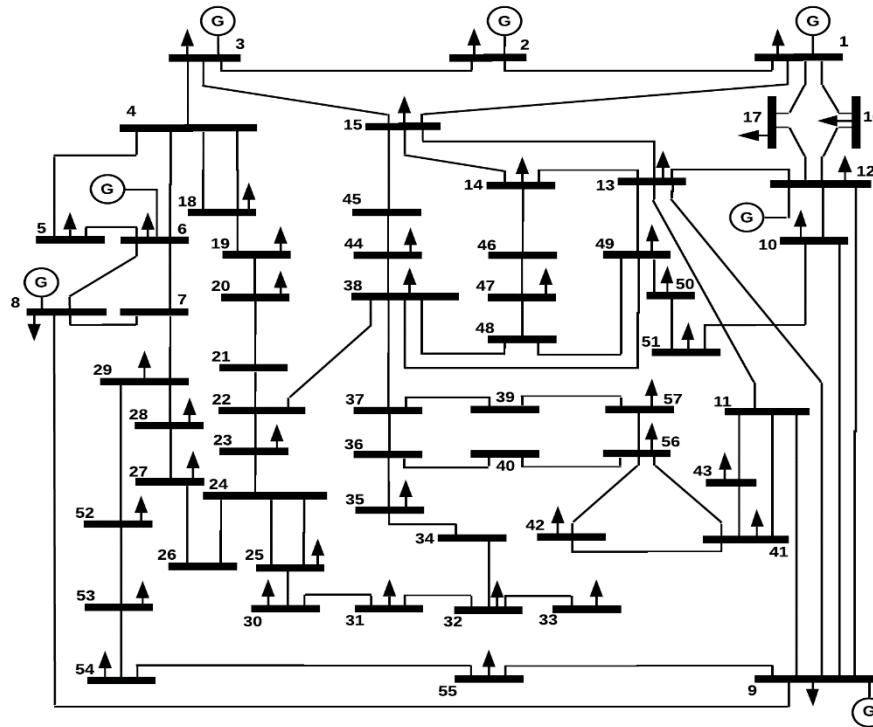
(i)



(j)



(k)



(l)

Figure 7 (a)~(l) Transmission restoration path from 1 p.u. time to 12 p.u. time

Figure 8 depicts the total generation and load pickup curves of the system when considering this base case scenario. Based on this figure, the demand loads are restored completely at 18 p.u. time. In other words, after a blackout occurs, the studied system can return back to the normal operation within 3 hours. As one can see, although the transmission network recovers at 12 p.u. time, the total restored load is 1002 MW until 16 p.u. time. As mentioned earlier, this is because two generators are not able to operate normally and supply power into the system, the amount of generation cannot satisfy the required demand load, and hence the full load outage recovery cannot be achieved earlier. When the remaining generators begin to offer generating power to the system at 16 p.u., the pickup loads continue to increase and reach the maximum at 18 p.u. time.

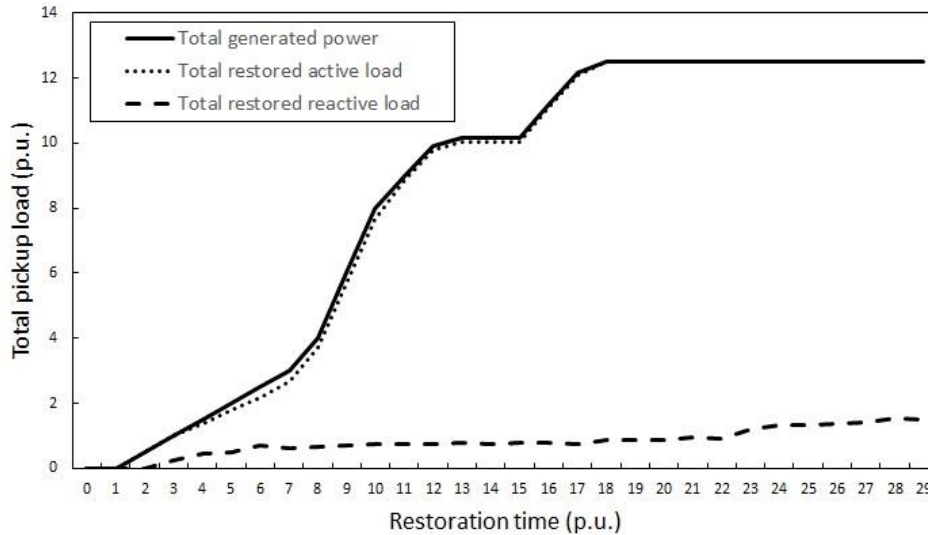


Figure 8 Total generated power and real and reactive load pickup in the base case scenario

3.4 Conclusion

An optimization model was formulated to simulate the process of restoration in transmission networks. The objective function in the model is to maximize the total

generation capacity and minimize the unserved loads. A generator start-up sequence and a transmission recovery path was established with constraints including initial conditions constraints, energization sequence constraints, components characteristics constraints, power balance constraints, and load pickup constraints.

After testing the proposed MILP optimization model on the IEEE 57 bus test system, an optimal generator start-up sequence, an optimal transmission recovery path and total load pickup time are achieved. The numerical results showed that it took 2 hours for the transmission system to recover, and the 3 hours for the entire system to return back to its normal operating condition.

Chapter 4: Incorporating Wind Energy in Power System Restoration

4.1 Introduction

Compared with conventional generators such as steam turbines and combustion turbines, wind turbines offer two main advantages: (i) they can reduce the cost of generation and (ii) ameliorate the environmental requirement. As the report mentioned in 2008 [31], the U.S. Department of Energy set a goal that wind energy supplies 20% of the country's electricity need in 2030. In 2018, wind power generated 6.5% of the nation's electricity demand [33]. Because wind power is increasing its penetration in electric power system, it is necessary for researchers to consider the impact of wind energy in power system operation and restoration.

This chapter will discuss the influences on power system restoration effectiveness when incorporating wind energy. The IEEE 57-bus system from Chapter 3 will be modified with introducing wind farms into the system. An optimization model is established to simulate the procedure of system restoration with wind farms. The result on the restoration efficiency will be then obtained. A sensitivity analysis is then presented in different cases of wind farms to further demonstrate the influence of wind energy in system restoration.

4.2 Problem Formulation

Here, an optimization model is established for system restoration incorporating wind farms. This model is similar to the model presented earlier in chapter 3, which is to maximize the total generation capacity and minimize the unserved load. The only

difference between these two models concerns with maximizing the total generation capacity. For wind farms, their capacity should be considered part of the total generation capacity. The model is shown below:

$$\max \left(\sum_{t \in T} \sum_{g \in G} (P_g^{\max} - P_g^{\text{start}}) n_{g,t} + \sum_{t \in T} \sum_{w \in W} P_{w,t}^{\text{fore}} n_{w,t} - \sum_{t \in T} \sum_{d \in D} \hat{\partial}_d (P_d^{\max} - P_{d,t}) \right) \quad (4.1)$$

Where, $P_{w,t}^{\text{fore}}$ denotes the wind farms' forecasted power at each time t and binary variable $n_{w,t}$ represents the status of wind farms. Similarly, initial conditions constraints, energization sequence constraints, components characteristics constraints, power balance constraints, and load pickup constraints should be involved in the optimization model for power grid restoration.

4.2.1 Initial Conditions Constraints

At the beginning, all components in the system are de-energized and BS generating units would begin the start-up procedure at the first unit of restoration time. Constraints (3.2) – (3.6) are still used here. In addition, constraint (4.2) shows that wind farm w is off at the beginning.

$$n_{w,t=0} = 0, \quad w \in W \quad (4.2)$$

4.2.2 Energization Sequence Constraints

There is an energization sequence for the transmission network. The components of the network should be energized from the buses connected to BS generating units step by step. Constraints (3.7) – (3.14) are still employed here. At this point, wind farm units need to be considered into the energization sequence. Wind turbines can be considered as

the BS and NBS generating units. In this thesis, we assume that wind generators are operated like NBS generating units. Constraint (4.3) illustrates that wind farm unit w cannot be started until the bus connected to it is energized.

$$n_{w,t} \leq n_{i,t}, \quad i \in B_w \quad (4.3)$$

4.2.3 Components Characteristics Constraints

All generators, transmission lines, and load demands have limitation, so constraints (3.15) – (3.22) are needed here. Additionally, the scheduled power of wind farms has a boundary as well, as enforced in constraint (4.4) and constraint (4.5). One difference between the wind generators and conventional generators is that wind generators have high ramping rates and can be started faster. Assuming the wind farms having a large ramping rate, there is no constraint to limit wind power ramping. In this thesis, the goal is to achieve a maximum wind utilization during the restoration process; so, it is assumed that the percentage of the utilized wind power would not decrease as time goes by, as shown in constraint (4.6).

$$0 \cdot n_{w,t} \leq P_{w,t} \leq P_{w,t}^{fore} n_{w,t} \quad (4.4)$$

$$0 \cdot n_{w,t} \leq Q_{w,t} \leq Q_{w,t}^{fore} n_{w,t} \quad (4.6)$$

$$P_{w,t} / P_{w,t}^{fore} \leq P_{w,t+1} / P_{w,t+1}^{fore} \quad (4.6)$$

4.2.4 Power Balance Constraints

Each bus should have real and reactive power balance between generating power and loads, as shown in (4.7) and (4.8). And the linearized AC power flow constraints are also set in (3.27) – (3.30).

$$\sum_{g \in G_i} (P_{g,t} - P_{g,t}^{start}) + \sum_{w \in W_i} P_{w,t} - \sum_{d \in D_i} P_{d,t} = \sum_{k \in K_f} P_{k,t} - \sum_{k \in K_r} P_{k,t} \quad (4.7)$$

$$\sum_{g \in G_i} Q_{g,t} + \sum_{w \in W_i} Q_{w,t} - \sum_{d \in D_i} Q_{d,t} = \sum_{k \in K_f} Q_{k,t} - \sum_{k \in K_i} Q_{k,t} \quad (4.8)$$

4.2.5 Load Pickup Constraints

Because the amount of wind power would be hard to predict and they change rapidly, we assume here that the wind farms do not have any contributions for dynamic reserve. Thus, load pickup constraints (3.31) and (3.32) are still valid.

4.3 Case Study

The test case here is the modified IEEE 57-bus test system similar to that introduced earlier in Chapter 3. A wind farm with 200 MW is installed at bus 38 (see Figure 9). In this case, the base power is assumed to be 100 MW and each restoration time step is 10 minutes (1 p.u.). Also, wind farm is operated at unity power factor, and the confidence interval for the wind farm output is set as 10% of the forecasted value. The formulated MILP model is simulated in the GAMS optimization platform.

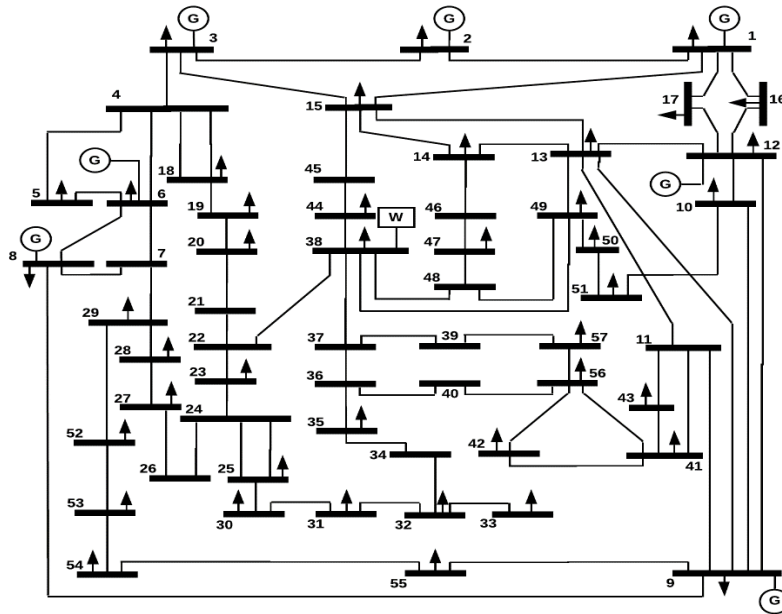


Figure 9 Modified IEEE 57-bus test system with a wind farm

After simulation of the restoration process, the generators start-up sequence and transmission recovery path in this case are achieved the same as those found in Chapter 3 under the based case scenario (see Figure 7). The total transmission network can be restored in around 2 hours. With the participation of the wind farm, the unserved loads can be supplied more than that in the based case at each time interval, as shown in Table 4.

Based on Figure 10, the total pickup load reaches 1192 MW at 12 p.u. which is the time that the total transmission network has recovered. The demand loads are restored completely at 16 p.u., which is 2 p.u. earlier than that in the base case scenario. Therefore, the participation of wind farms is beneficial in the system restoration process. Wind farms in the system can reduce the restoration time and increase the pickup loads at each recovery time step, thereby helping achieve an enhanced resilience.

Table 4 The Amount of Pickup Loads at Each Time Step in the Case with Wind

T (p.u.)	1	2	3	4	5	6
Total Demands (MW)	1250	1250	1250	1250	1250	1250
Restored Loads (MW)	0	50	99	137	181	296
Outages (MW)	1250	1200	1151	1113	1069	954
T (p.u.)	7	8	9	10	11	12
Total Demands (MW)	1250	1250	1250	1250	1250	1250
Restored Loads (MW)	457	573	769	966	1102	1192
Outages (MW)	783	677	481	284	148	58

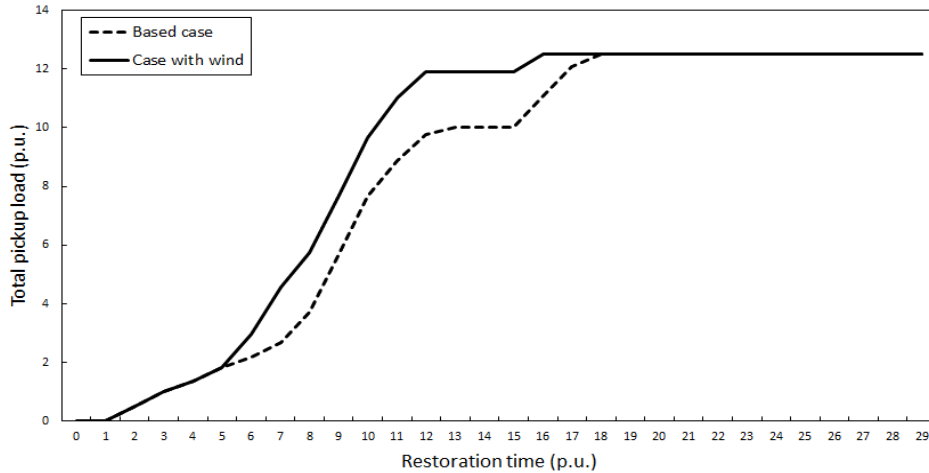


Figure 10 Total load pickup in the case with wind farm at bus 38

4.4 Sensitivity Analysis

4.4.1 Impact of Wind Power Penetration

In previous study case, the capacity of the installed wind farm was set as 200 MW, which represents 16% penetration. Here, the impact of different wind power penetration levels, including 8% (100 MW), 24% (300 MW), and 32% (400 MW), are discussed.

Figure 11 shows the curves of the total load pickup in different wind penetration scenarios. According to this figure, it is illustrated that the higher penetration of wind power can restore the system faster. As one can see, the load demands recover completely at 17 p.u. time in 8% penetration case, while at 16 p.u. time in 16% penetration case. Both 24% and 32% penetration of wind power can restore the system at 12 p.u. time. In these two penetration cases, when the transmission network is restored, the total demands would be resupplied immediately. Thus, higher penetration of wind farm can improve the system capability for a timely restoration and enhanced resilience.

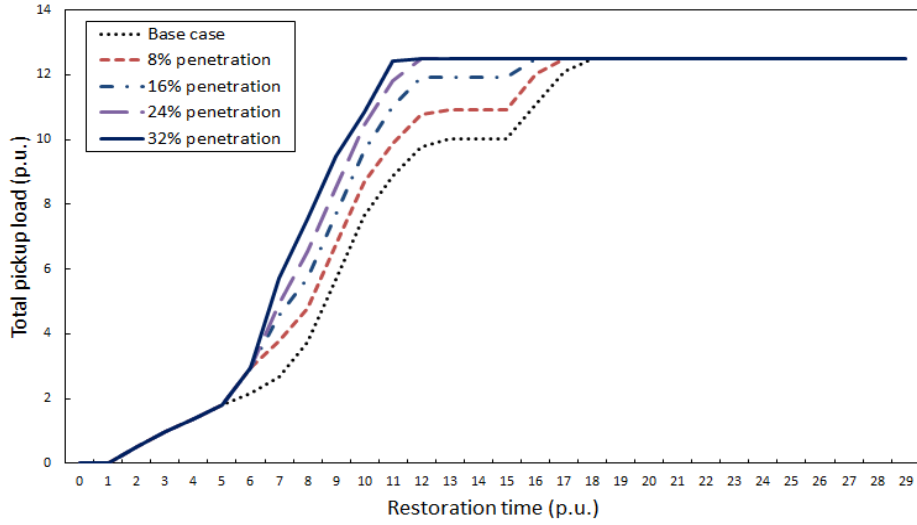
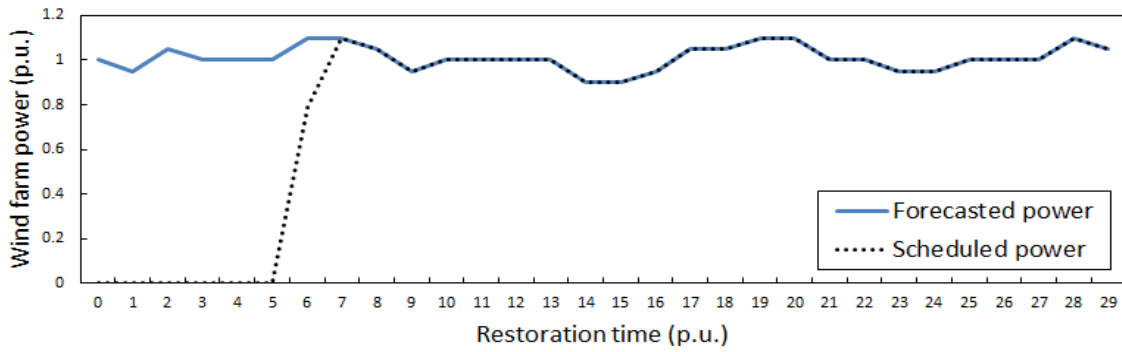
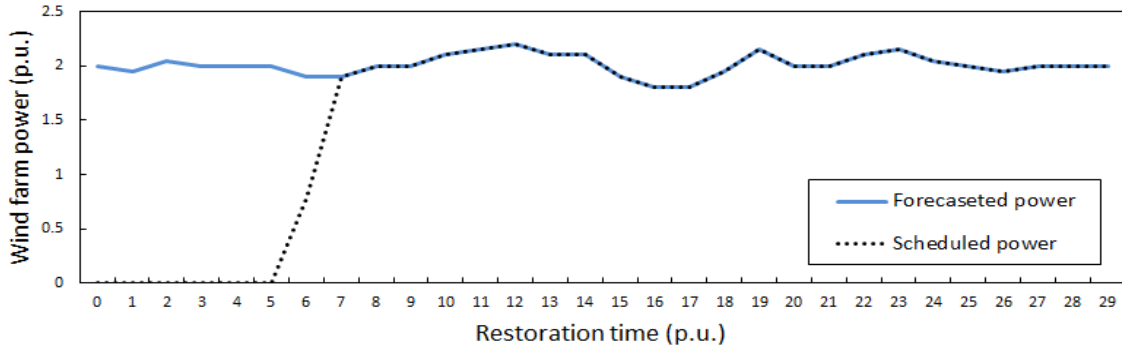


Figure 11 Total load pickup with different wind penetration levels



(a) 8% penetration



(b) 16% penetration

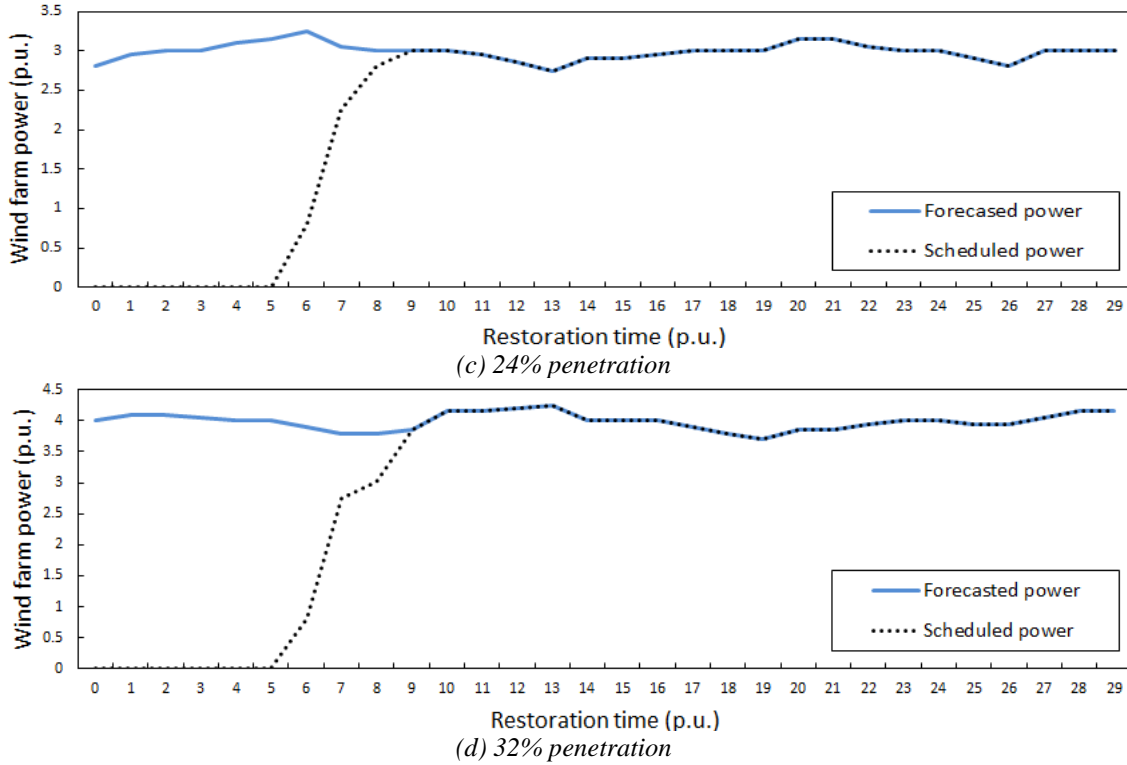


Figure 12 (a) ~ (d) Wind power with different penetration of wind farms

Figure 12 illustrates the relationship between the forecasted and scheduled power of a wind farm with different capacities. Because the real and reactive power generated should be balanced with those of loads, the output power of the wind farm cannot immediately reach its forecasted power. For the 100 MW or 200 MW capacity wind farm, it took around 2 p.u. time to supply 100 percent of the forecasted power. The 300 MW or 400 MW capacity wind farm spent nearly 3 p.u. on providing the entire forecasted power. Therefore, a large amount of wind energy is curtailed. The more capacity a wind farm owns, the larger wind energy curtailment will be resulted.

4.4.2 The Impact of the Wind Farm's Location

In this section, we discuss the influence of the installed location of the wind farm in the network on the restoration efficiency. Besides the original location at bus 38, we will

investigate a random location of the wind farm at buses 16, 25 and 29. The capacity of the wind farm is 200 MW. After simulation, the optimization results reveal that the wind farm's location in the network has a direct impact on the restoration process, as shown in Figure 13.

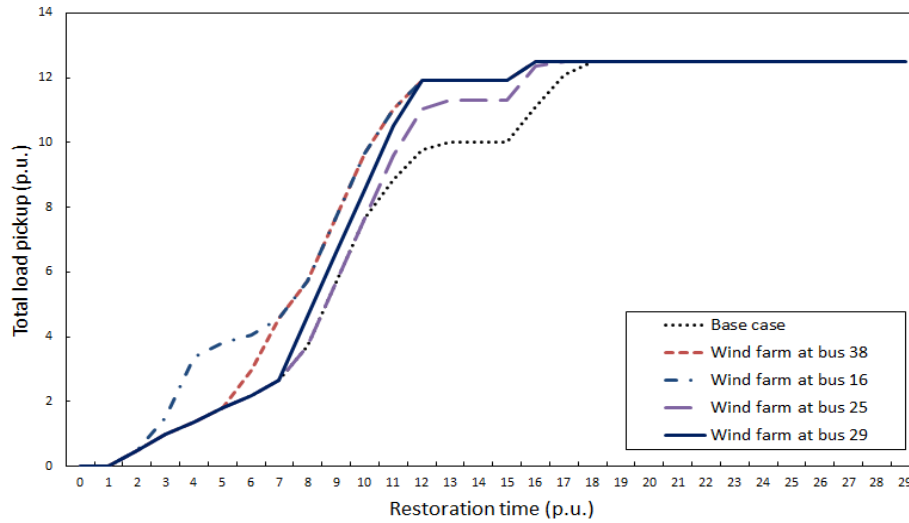
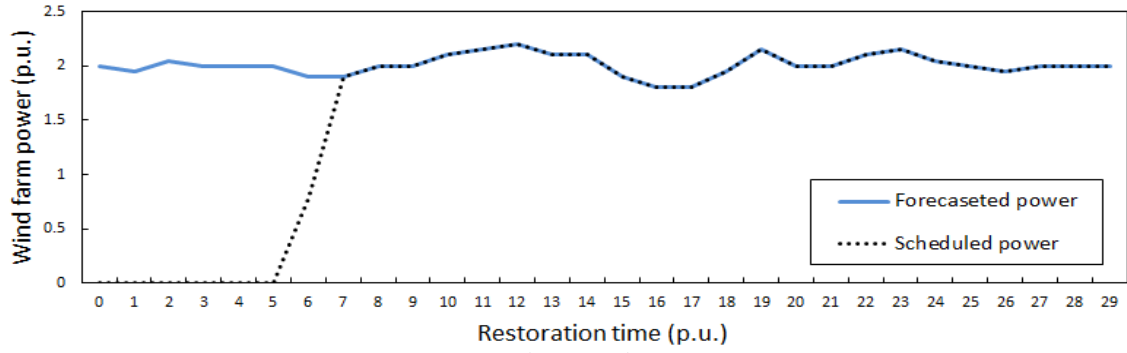
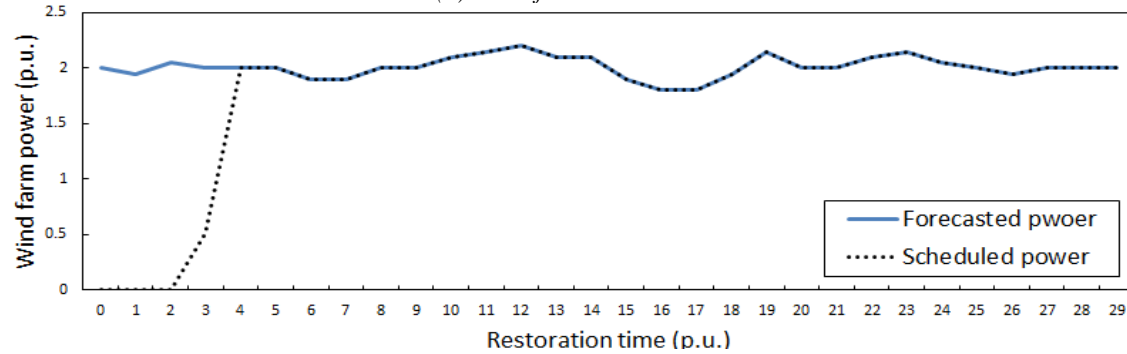


Figure 13 Total load pickup at different location of the wind farm

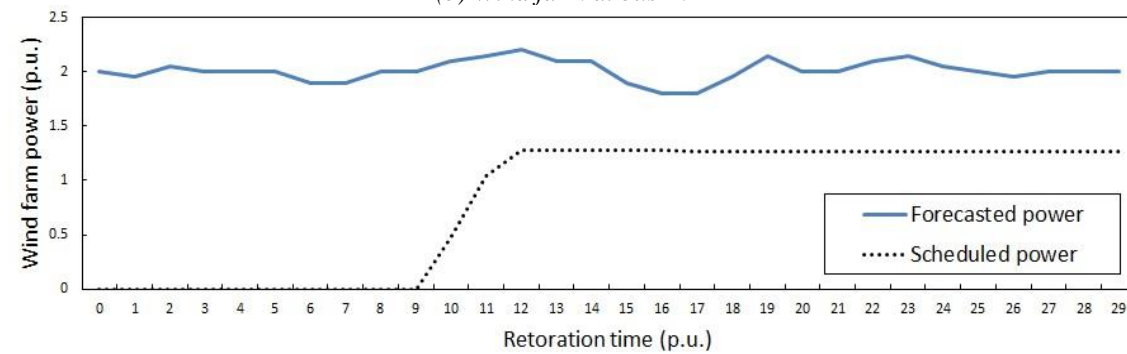
According to Figure 13, different locations for the wind farms have different impacts on the amount of pickup load at each restoration time unit. The system recovers completely at 16 p.u. in all different location test cases. Because the bus 16 is energized faster than the others, the wind farm at bus 16 supplies energy to the system fastest. Hence, at the early restoration period, the system with the wind farm located at bus 16 can restore more loads than the wind farm at other locations.



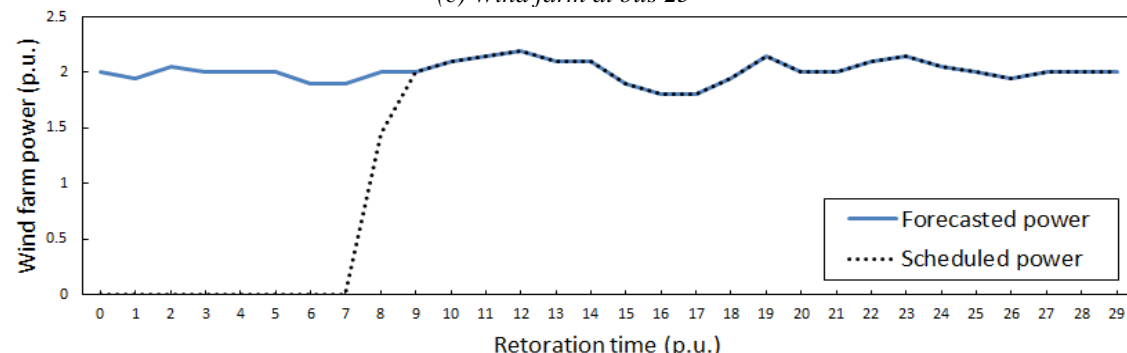
(a) Wind farm at bus 38



(b) Wind farm at bus 16



(c) Wind farm at bus 25



(d) Wind farm at bus 29

Figure 14 (a) ~ (d) Wind farm power at different locations

Figure 14 depicts the forecasted and scheduled power of the wind farm at different locations. In all cases, the amount of scheduled power cannot increase to that of the forecasted immediately. Because of the limitation arisen from the system's components, the wind farm at bus 25 only provides 126 MW power, while its forecasted power is 200 MW. Based on the results in Figure 14, the wind farm located at the earlier energized buses can reduce wind energy spillage. Thus, the wind farm's location also has a direct impact on the wind energy curtailment.

4.4.3 The Impact of Wind Farms' Quantity

The analysis mentioned above was on the impact of one wind farm for system restoration. The analysis for wind energy in this section is focused on two or three wind farms in the system. For better comparison, we assume the following three scenarios. The first scenario is to have one 100 MW wind farm at bus 15 and one 100 MW wind farm at bus 38. The second scenario is setting a 200 MW wind farm at bus 15 and a 100 MW wind farm at bus 38. The third scenario is to have a 100 MW wind farm at bus 10, a 100 MW wind farm at bus 15, and a 100 MW wind farm at bus 38. After simulating these three scenarios and running the optimization model, the amount of pickup loads at each restoration time step is obtained and shown in Figure 15.

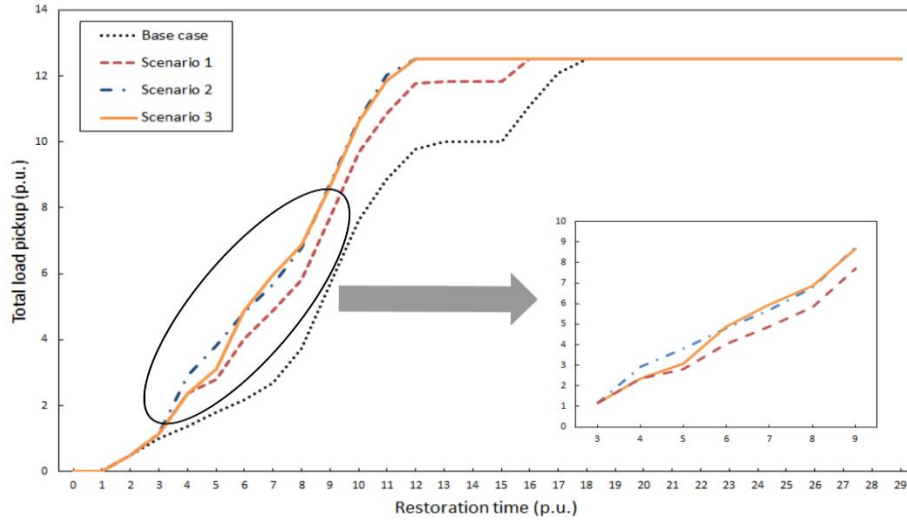
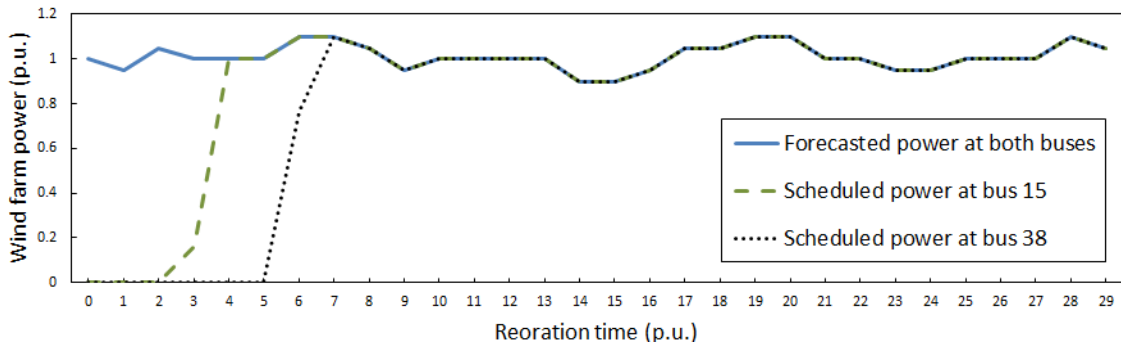
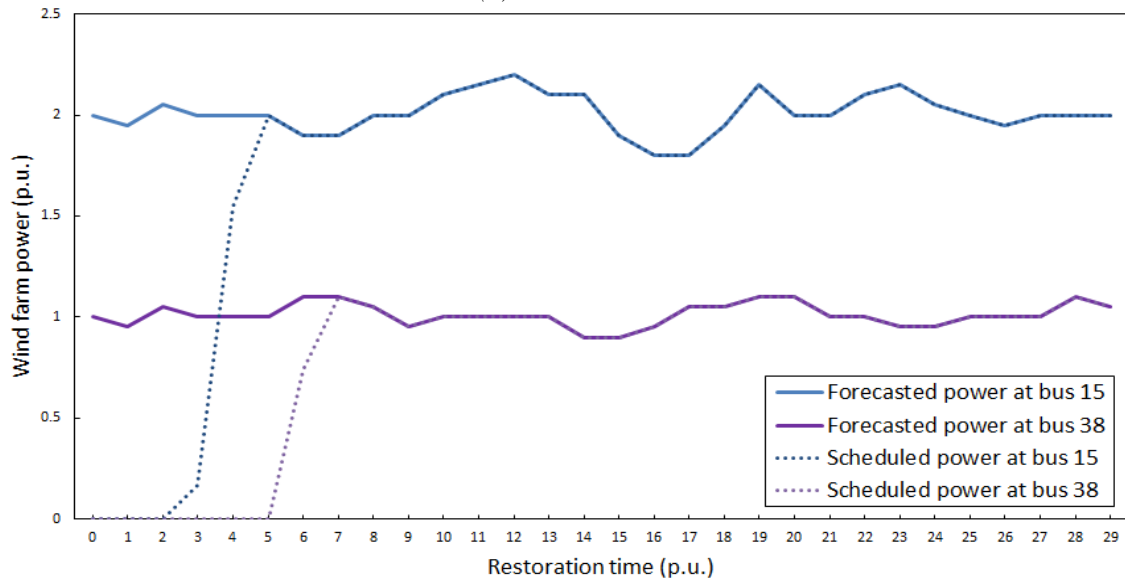


Figure 15 Total load pickup with different number of wind farms



(a) Scenario 1



(b) Scenario 2

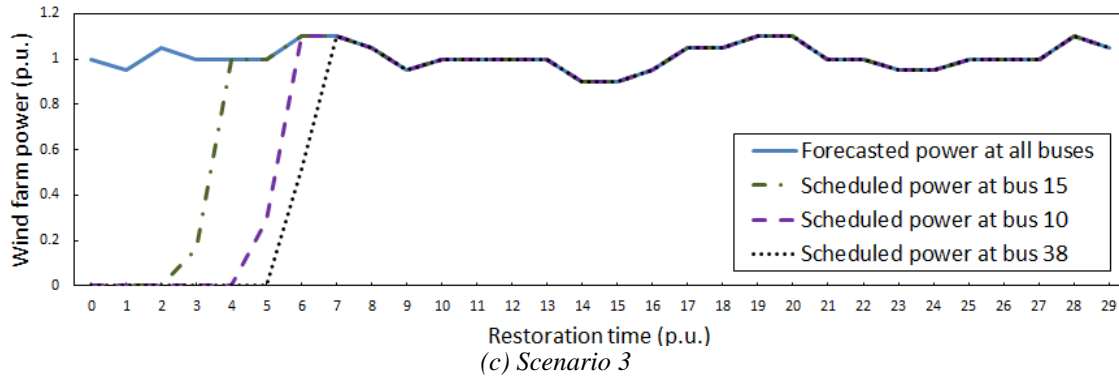


Figure 16 (a) ~ (c) Wind power with different number of wind farms

According to the Figure 15, increasing the number of the wind farms can have a positive impact on system restoration. Compared with the base case scenario studied earlier, installing more than one wind farm into the system can shorten the restoration time. At the early restoration time periods, the system in scenario 2 could recover more demand loads than other two scenarios, but it has more wind curtailment than other two scenarios, as shown in Figure 16.

4.5 Conclusion

In this chapter, the impact of wind energy on the system restoration has been discussed. Because wind power is intermittent and can highly fluctuate and since they are attributed a large ramping rate, they are able to supply energy and assist the system operation and restoration in a shorter time period. Based on this characteristic, we established an MILP-based optimization model applied to the modified IEEE 57-bus system to simulate the procedure of the system restoration with wind farms.

Assuming a 200 MW wind farm as a NBS generating unit, the generator start-up sequence and the transmission recovery path in this situation were observed similar to the

sequence and the path in the base case scenario without wind power (studied in Chapter 3). Compared with the system without a wind farm, all loads are restored faster in the system with a wind farm. Hence, wind power is beneficial to the system restoration.

The sensitivity analysis on the influence of wind energy was also discussed in this chapter. The analysis involved the impact of wind power penetration, the impact of the wind farm's location, and the impact of the wind farms' quantity. With high wind power penetration, the system restoration time can be shortened. Based on the transmission recovery path, different settings on the locations of the wind farm have different contribution to the system restoration. The more wind farms participating into the restoration process, the more loads are restored at each restoration time, thereby achieving an enhanced overall resilience.

Chapter 5: Coordination of Wind Power and PSH for System Restoration

5.1 Introduction

Pumped-storage hydro (PSH) is a type of hydroelectric energy storage [129]. It consists of two water reservoirs at different elevations. PSH can utilize hydro turbines to generate power (discharge) as water moves down from upper reservoirs, while it can consume electric power from external systems to pump the water (recharge) to upper reservoir (see Figure 17). PSH is a proven, reliable, and commercially available large-scale energy storage resource, which provides 97% of the total utility-scale electricity storage in the United States as of 2015 [130]. In addition, PSH offers a number of services and contributions to the power system, such as frequency regulation, contingency reserves, voltage support, and others [131]. With the increasing penetration of renewable resources, PSH can also be employed to balance the daily loads and variable generation from renewable resources on the grid.

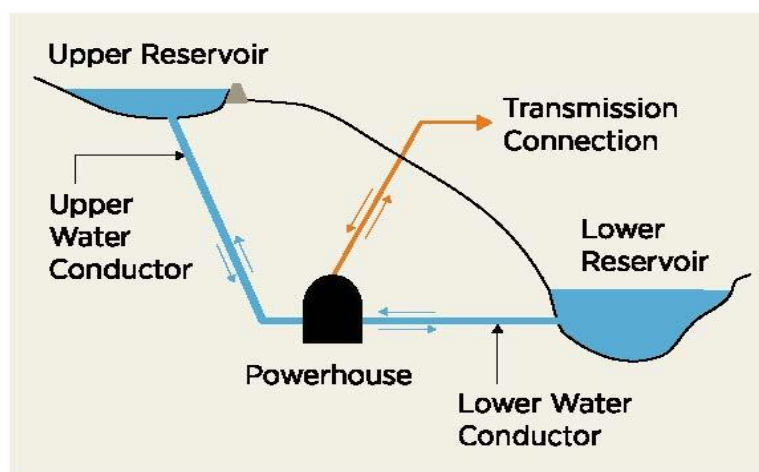


Figure 17 Typical configuration of a pumped storage hydropower plant [131].

With these characteristics, it is beneficial to utilize PSH in the system restoration process. In this chapter, the influence of coordinating wind energy and PSH for the system restoration is analyzed. The IEEE 57-bus system from Chapter 4 will be modified with introducing PSH into the system. The optimization model derived in Chapter 4 will be extended to simulate the restoration process with PSH. Then, several case studies will be analyzed on the impact of PSH on the restoration and on reducing wind curtailment.

5.2 Problem Formulation

The formulation in this chapter is derived from Chapter 4, so the objective function in the optimization model is the same as that in Chapter 4, as shown below:

$$\max \left(\sum_{t \in T} \sum_{g \in G} (P_g^{\max} - P_g^{\text{start}}) n_{g,t} + \sum_{t \in T} \sum_{w \in W} P_{w,t}^{\text{fore}} n_{w,t} - \sum_{t \in T} \sum_{d \in D} \partial_d (P_d^{\max} - P_{d,t}) \right) \quad (5.1)$$

Similarly, the model here also process initial conditions constraints, energized sequence constraints, components characteristics constraints, power balance constraints, and pickup load constraints. Moreover, to simulate the restoration process with PSH, PSH constraints are required to be added in the optimization model.

5.2.1 Initial Conditions Constraints

Based on the assumptions taken in this thesis, a severe blackout results in the entire system being de-energized with no physical damage on the system components. Constraints (3.2) – (3.6), (4.2) are needed here. Additionally, there is a constraint (5.2) showing the initial status of a PSH unit.

$$n_{h,t=0} = 0, \quad h \in H \quad (5.2)$$

5.2.2 Energization Sequence Constraints

To simulate the restoration process in the optimization model, energization sequence constraints (3.7) – (3.14) and (4.3) should be considered. Although a PSH unit can operate as either a BS generating unit or a NBS generating unit, we first consider the PSH unit as a NBS unit in this analysis. The PSH unit cannot be started until the bus connected to it is energized, as shown in (5.3).

$$n_{h,t} \leq n_{i,t}, \quad i \in B_h \quad (5.3)$$

5.2.3 Components Characteristics Constraints

All generators, transmission lines, and load demands have limitations to be satisfied, thus constraints (3.15) – (3.22) and (4.4) – (4.6) are needed. The characteristics of a PSH unit will be presented within the PSH constraints.

5.2.4 Power Balance Constraints

Each bus should have real and reactive power balance between generating power and loads, as shown in (5.4) and (5.5). And the linearized AC power flow constraints are also presented in (3.27) – (3.30).

$$\sum_{g \in G_i} (P_{g,t} - P_{g,t}^{start}) + \sum_{w \in W_i} P_{w,t} + \sum_{h \in H_i} P_{h,t} - \sum_{d \in D_i} P_{d,t} = \sum_{k \in K_f} P_{k,t} - \sum_{k \in K_t} P_{k,t} \quad (5.4)$$

$$\sum_{g \in G_i} Q_{g,t} + \sum_{w \in W_i} Q_{w,t} - \sum_{d \in D_i} Q_{d,t} = \sum_{k \in K_f} Q_{k,t} - \sum_{k \in K_t} Q_{k,t} \quad (5.5)$$

5.2.5 Load Pickup Constraints

When a PSH is in its generation mode, it operates as a hydropower plant. As a result, PSH has contribution to increasing the load pickup capacity, as shown in constraint (5.6).

Constraint (3.32) is also required to be satisfied.

$$\sum_{d \in D} P_{d,t+1} - \sum_{d \in D} P_{d,t} \leq \sum_{g \in G} \lambda_g P_{g,t} + \sum_{h \in H} \lambda_h P_h^{g,\max} \quad (5.6)$$

5.2.6 PSH Constraints

Generally, for a hydro unit, the relationship between the head of associated reservoir, the water discharged, and the power generated is non-linear and non-concave [132]. The output power of the PSH would be formulated as a non-linear and non-convex function of the turbine discharge rate and the net head [133]. In this thesis, variations on the net water head are ignored, because it is assumed that each PSH unit has one water-to-power curve for the generation mode and on power-to-water curve for the pumping mode in [134]. Thus, two binary variables $S_{h,t}^g$, $S_{h,t}^p$ are introduced to represent that the PSH unit h is in generation and pumping modes, respectively. These modes are mutually exclusive in each restoration time, and cannot operate until PSH unit h is started, as shown in (5.7). Constraint (5.8) illustrates the net output power of the PSH. In addition, the generation and pumping mode capacity of the PSH should be restricted by its limitation, as shown in (5.9) and (5.10).

$$S_{h,t}^g + S_{h,t}^p \leq n_{h,t} \quad (5.7)$$

$$P_{h,t} = P_{h,t}^g - P_{h,t}^p \quad (5.8)$$

$$P_h^{g,\min} S_{h,t}^g \leq P_{h,t}^g \leq P_h^{g,\max} S_{h,t}^g \quad (5.9)$$

$$P_h^{p,\min} S_{h,t}^p \leq P_{h,t}^p \leq P_h^{p,\max} S_{h,t}^p \quad (5.10)$$

Besides net output power of the PSH unit that is constrained, the reservoir volume is also limited, as shown in constraint (5.11). When the PSH begins to discharge, reservoir volume would decrease. Constraint (5.12) presents the relationship between net discharge rate and reservoir volume. The net discharge rate is shown in constraint (5.13). Similarly, discharge rate and recharge rate have their limitation, as shown in (5.14) and (5.15).

$$Vol^{\min} \leq Vol_t \leq Vol^{\max} \quad (5.11)$$

$$Vol_{t+1} = Vol_t - q_{h,t} \Delta T \quad (5.12)$$

$$q_{h,t} = q_{h,t}^g - q_{h,t}^p \quad (5.13)$$

$$q_h^{\min} S_{h,t}^g \leq q_{h,t}^g \leq q_h^{\max} S_{h,t}^g \quad (5.14)$$

$$q_h^{\min} S_{h,t}^p \leq q_{h,t}^p \leq q_h^{\max} S_{h,t}^p \quad (5.15)$$

5.3 Case Study

In this chapter, the test case is the modified IEEE 57-bus similar to the system in presented earlier in Chapter 4. In different cases, I will set a PSH unit in different locations. The data corresponding to the PSH unit is presented in Appendix 3. The restoration process, the MILP optimization model in which the wind energy and PSH is coordinated, is simulated in the GAMS optimization platform.

5.3.1 Case 1

In this case, the test system configuration is based on the one presented in Chapter 4, which has a 200 MW wind farm located at bus 38. In addition, the PSH unit is set to be at bus 38 as well (see in Figure 18).

After simulation, the obtained generation start-up and transmission recovery sequences are the same as the sequences in Chapter 4. It took 12 p.u. time interval to recover the entire transmission network. Compared with the system without PSH, the system restoration time with PSH would decrease. All loads in the system can be restored within around 12 p.u. time, as shown in Figure 19.

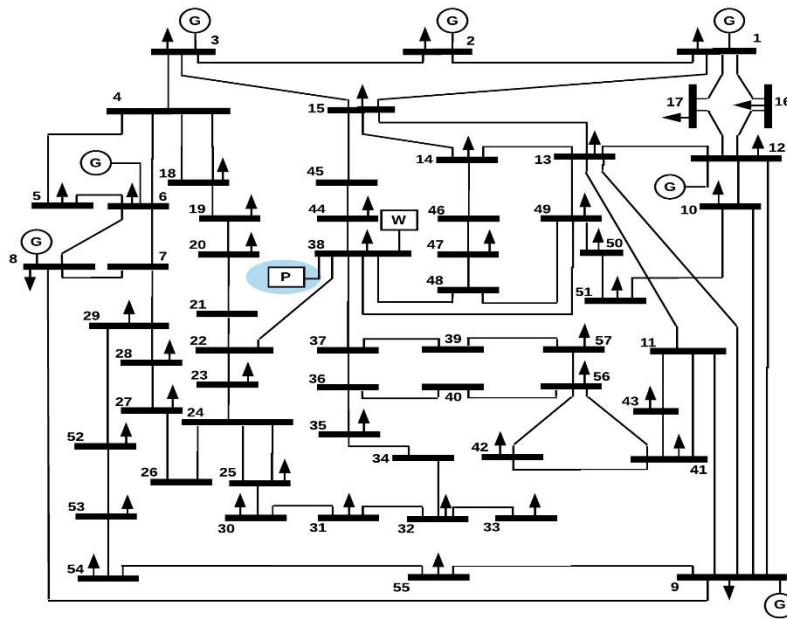


Figure 18 Modified IEEE 57-bus test system with a PSH located at bus 38

According to Figure 20, with the help of PSH, the scheduled output of the wind farm can reach its forecasted power faster than the system without PSH. The shadow in the figure illustrates the realized reduction in wind curtailment. In this case, the amount of wind curtailment can be decreased by 6.67GWh. This power is utilized by PSH for pumping water from lower to upper reservoir. Based on the numerical results of our simulations, Table 5 shows the operation modes of PSH during the restoration period.

Assuming the initial reservoir volume to be 3.2 Hm^3 , Figure 21 depicts the change in reservoir volume during the restoration process.

Table 5 Operating Modes of PSH in Case 1

Time (p.u.)	1	2	3	4	5	6	7	8	9	10	11	12
Gen. mode	0	0	0	0	0	0	1	1	1	1	1	1
Pump. mode	0	0	0	0	0	1	0	0	0	0	0	0

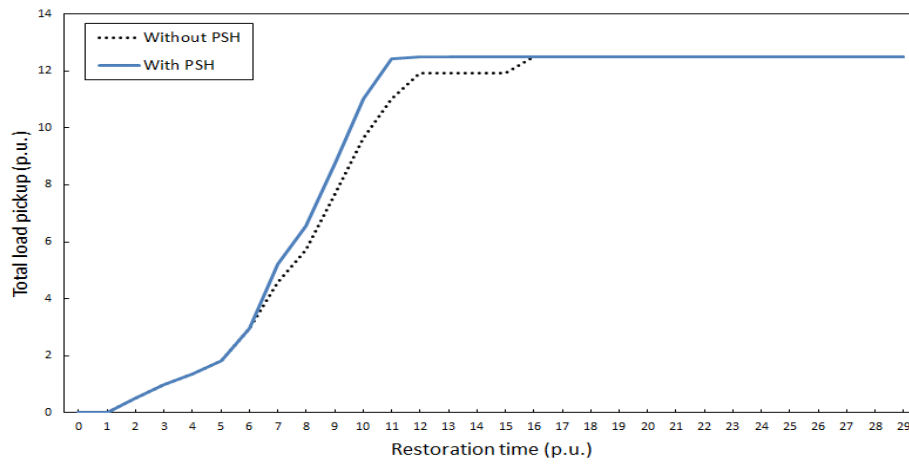


Figure 19 Total load pickup with PSH located at bus 38

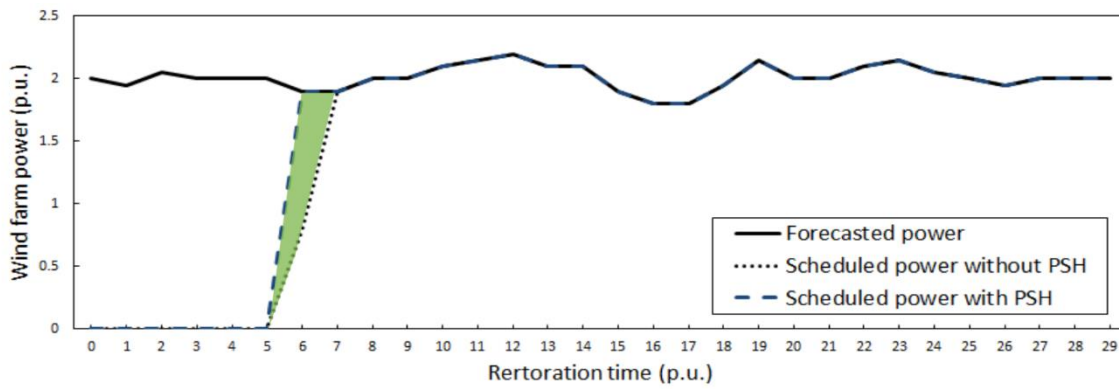


Figure 20 Forecasted and scheduled wind power in Case 1

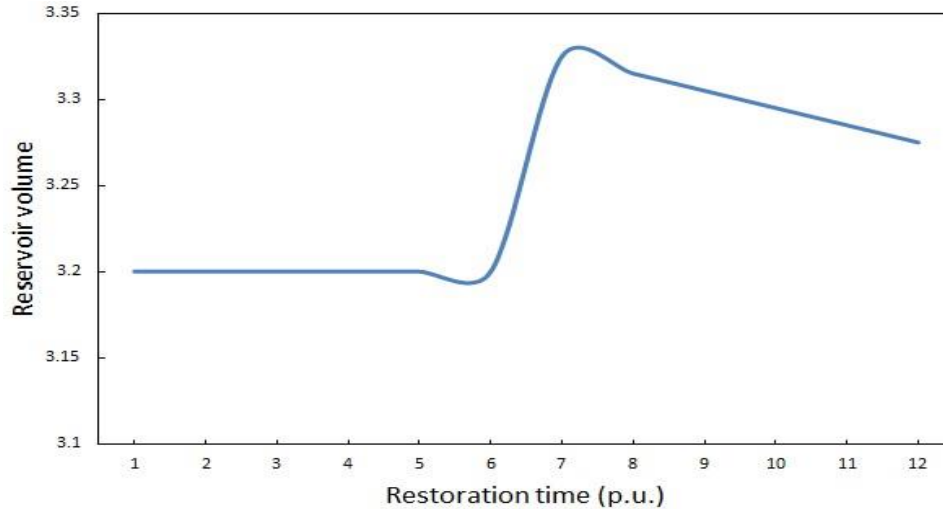


Figure 21 Reservoir volume of PSH

According to the results tabulated in Table 5 and demonstrated in Figure 21, the PSH is in pumping mode at 6 p.u. time and in generation mode from 7 p.u. to 12 p.u. time periods. At the 6 p.u. time, PSH unit pumped water from the lower to upper reservoir by using the energy produced by the wind farm. The wind energy employed for pumping would be curtailed to keep security of the system in the case without the PSH unit. When the wind power output reaches its forecasted power, the PSH unit is then in generation mode and generate electricity through allowing water to fall from upper to lower reservoir. The power produced by the PSH unit can assist the system to recover soon. Thus, the PSH unit can indirectly help increase the efficiency of wind energy for system restoration.

5.3.2 Case 2

As we can see in Figure 14 (c), if a wind farm is located at bus 25, it would cause a large amount of wind curtailment. In this case, the PSH unit is assumed to be located at bus 25 with the wind farm. As shown in Figure 22, the shadow presents the amount of

reduction in wind curtailment. With the help of the PSH unit, the wind farm can reduce a large number of wind energy curtailment.

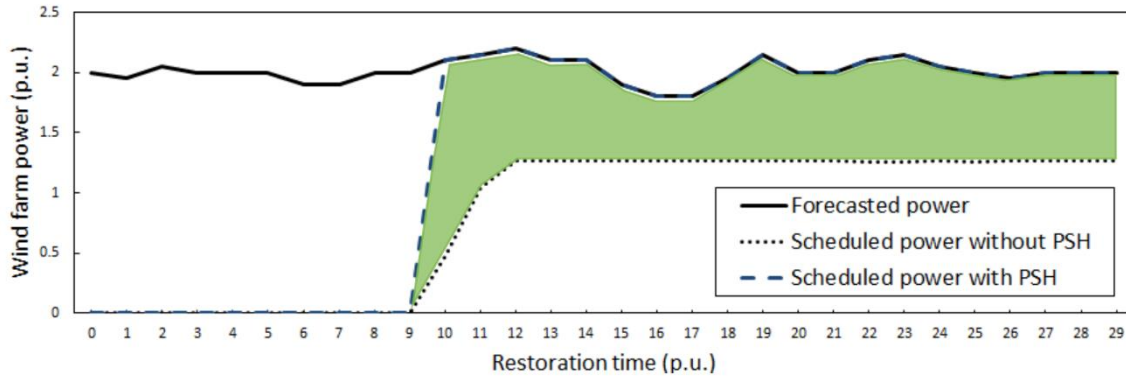


Figure 22 Forecasted and scheduled wind power in Case 2

According to Table 6, the PSH unit is in pumping mode in the entire restoration process. The PSH consumes the wind energy to pump water from lower to upper reservoir. This energy is transferred as water volume stored in upper reservoir.

Table 6 Operating Modes of PSH in Case 2

Time (p.u.)	1	2	3	4	5	6	7	8	9
Gen. mode	0	0	0	0	0	0	0	0	0
Pump. mode	0	0	0	0	0	0	0	0	0
Time (p.u.)	10	11	12	13	14	15	16	17	18
Gen. mode	0	0	0	0	0	0	0	0	0
Pump. mode	1	1	1	1	1	1	1	1	1

5.3.3 Case 3

Because the PSH unit operates like a hydropower plant in generation mode, it can be functioned as a BS generating unit. In this case, the impact of the PSH operating as a

BS unit for the system restoration is discussed. In the test system, a PSH unit is assumed to be located at bus 29 (see Figure 23).

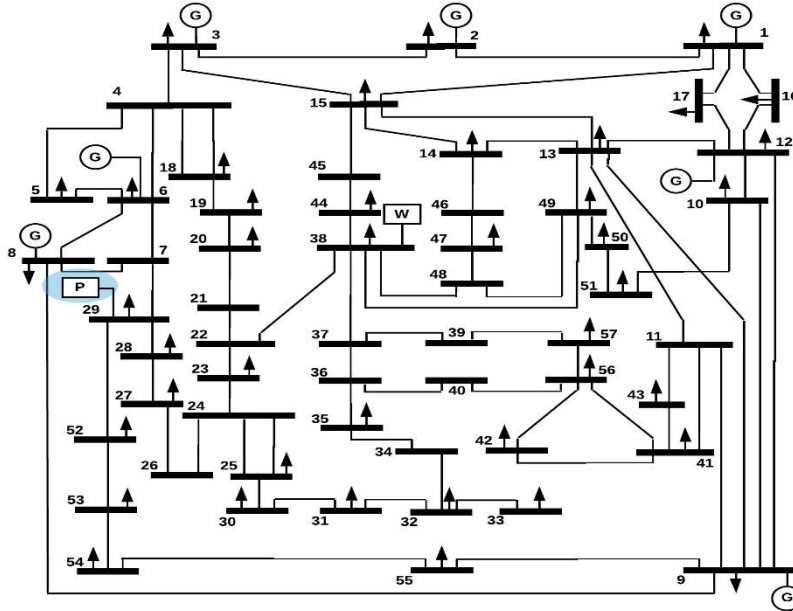


Figure 23 Modified IEEE 57-bus system with PSH located at bus 29

Because the PSH unit operates as a BS unit, the bus connected to it would be energized after it starts to generate power. Constraint (5.3) should be then replaced by constraint (5.16):

$$n_{h,t} \geq n_{i,t}, \quad i \in B_h \quad (5.16)$$

After simulating the optimization model in GAMS, a new generator start-up and transmission recovery sequence would be obtained. Table 7 shows the optimal start-up time for generators, while Table 8 and Table 9 illustrate the energized time of transmission buses and lines. Based on the numerical results presented in these tables, it took less time to recover the entire transmission network. In the base case scenario, the transmission network need to spend 12 p.u. time to be fully restored. In this case, the entire transmission

network can be restored within 11 p.u. time. Therefore, the PSH operating as a BS unit is beneficial to recover the transmission network during restoration period.

Table 7 Optimal Start-up Time for Generators

Gen. No.	Time (p.u.)	Type	Gen. No.	Time (p.u.)	Type
G1	2	Hydro turbine	G5	16	Steam turbine
G2	9	Steam turbine	G6	8	Steam turbine
G3	10	Steam turbine	G7	16	Combustion turbine
G4	7	Combustion turbine			

Table 8 Energized Time of all Buses

Bus	1	2	3	4	5	6	7	8	9	10
Time (p.u.)	2	3	4	5	5	4	3	4	5	5
Bus	11	12	13	14	15	16	17	18	19	20
Time (p.u.)	6	4	4	4	3	3	3	6	7	8
Bus	21	22	23	24	25	26	27	28	29	30
Time (p.u.)	8	7	7	6	7	5	4	3	2	8
Bus	31	32	33	34	35	36	37	38	39	40
Time (p.u.)	9	10	11	10	9	8	7	6	8	9
Bus	41	42	43	44	45	46	47	48	49	50
Time (p.u.)	7	8	7	5	4	5	6	6	5	6
Bus	51	52	53	54	55	56	57			
Time (p.u.)	6	3	4	5	6	8	9			

Table 9 Energized Time of all Transmission Lines

Bus	1	2	3	4	5	6	7	8	9	10
Time (p.u.)	3	4	5	6	5	4	5	5	6	6
Bus	11	12	13	14	15	16	17	18	19	20
Time (p.u.)	5	5	5	4	3	3	3	4	6	6
Bus	21	22	23	24	25	26	27	28	29	30
Time (p.u.)	5	4	5	6	5	4	4	4	7	8
Bus	31	32	33	34	35	36	37	38	39	40
Time (p.u.)	9	8	8	7	7	7	6	5	4	3
Bus	41	42	43	44	45	46	47	48	49	50
Time (p.u.)	3	8	9	10	11	11	10	9	8	7
Bus	51	52	53	54	55	56	57	58	59	60
Time (p.u.)	8	9	7	7	8	8	6	4	5	7
Bus	61	62	63	64	65	66	67	68	69	70
Time (p.u.)	7	6	6	7	6	5	3	4	5	6
Bus	71	72	73	74	75	76	77	78	79	80
Time (p.u.)	7	5	9	8	9	9	9	6	7	6

Figure 24 illustrates the total load pickup curves for the studied system with and without the PSH unit during the restoration period. There is a strong evidence that the PSH operating as a BS unit can directly shorten the restoration time. In the system without the PSH unit, all loads require 16 p.u. time periods to recover, which it is 5 p.u. time later than that in the system with the PSH unit. Table 10 shows the amount of pickup loads at each time step. Therefore, the PSH unit can improve the capability of system restoration.

Table 10 The Amount of Pickup Loads at Each Time Step in Case 3

T (p.u.)	1	2	3	4	5	6
Total Demands (MW)	1250	1250	1250	1250	1250	1250
Restored Loads (MW)	0	67	116	303	347	479
Outages (MW)	1250	1183	1134	947	903	771
T (p.u.)	7	8	9	10	11	12
Total Demands (MW)	1250	1250	1250	1250	1250	1250
Restored Loads (MW)	695	861	1012	1177	1250	1250
Outages (MW)	555	389	238	73	0	0

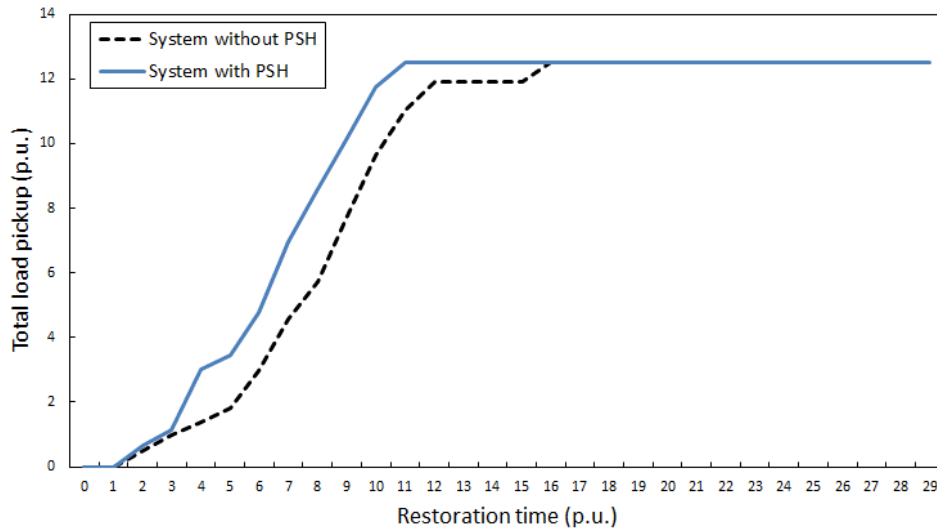


Figure 24 Total load pickup in Case 3

In this case, the PSH unit is in generation mode during the restoration process, as shown in Table 11.

Table 11 Operating Modes of PSH in Case 3

Time (p.u.)	1	2	3	4	5	6	7	8	9
Gen. mode	0	1	1	1	1	1	1	1	1
Pump. mode	0	0	0	0	0	0	0	0	0
Time (p.u.)	10	11	12	13	14	15	16	17	18
Gen. mode	1	1	1	1	1	1	0	0	0
Pump. mode	0	0	0	0	0	0	0	0	0

5.4 Conclusion

In this chapter, the impact of coordination of wind farm and PSH units for the system restoration has been discussed. PSH units can operate flexibly, because they offer two operating modes: generation mode and pumping mode. With this characteristic, PSH units not only can supply electricity to assist the system restoration, but also store spillage energy produced by wind farms. To simulate the restoration process with the help of a PSH unit, a MILP optimization model is established which includes the initial conditions constraints, energized sequence constraints, components characteristics constraints, power balance constraints, load pickup constraints, and PSH constraints.

The formulation is simulated on three tests cases. The first case is when a wind farm and a PHS unit are located at bus 38 together. The result presents that the PSH unit can reduce the wind energy curtailment at the early restoration period, and generate power to assist the restoration after the wind farm has provided the full energy. The second case is setting a wind farm and a PSH unit at bus 25 together. In this case, the PSH is in pumping

mode during the whole restoration process, and has reduced the wind curtailment significantly. The third case is having a PSH unit at bus 29. In this case, the PSH unit operates as a BS unit. The system can be restored fast with the PSH in this case. These three case studies have all proven that the PSH can ameliorate the system restoration capability directly and significantly, thereby helping achieve and enhanced grid reliability and resilience characteristics.

Chapter 6: Conclusion

6.1 Conclusion

It is more and more important to increase the efficiency and effectiveness of the system restoration, because large-scale load outages become more commonplace. There are extensive literature studying different applications, methods or techniques for the system restoration. In this thesis, a restoration strategy based on the black-start (BS) generating units is proposed. Cooperating wind energy and pumped-storage hydro (PSH) units, the restoration capability after a blackout has been presented and extensively analyzed. A mixed-integer linear program (MILP) optimization model is established to simulate the restoration process.

The simulation model aims to maximize the generation capability and minimize the load shedding. With several constraints, the model can present the logical moving path for power flow in the system. The MILP model is solved in the GAMS optimization platform.

After simulating the restoration process on the IEEE 57-bus test system, the total restoration time is found 3 hours in the base case scenario without any help or contribution from the wind energy and PSH unit. The optimal generator start-up and transmission recovery sequence was obtained. It took 2 hours for the system to recover its transmission network. In addition, the restoration capability has been improved significantly with the participation of wind energy. When a wind farm is installed in the system, the entire system can only be restored in a maximum of 160 minutes. With the increase in wind energy penetration level in the system, it took less time to recover the system. When the penetration is greater than 24%, the system only needs 2 hours to be restored completely.

Different locations and number of wind farms can also affect the restoration time. However, the simulation result showed that there is a disadvantage for utilizing wind farms in some scenarios. In order to keep the system security, the available wind energy could be highly and maximally used for the system restoration. A large number of wind curtailment exists. To address this problem, PSH is introduced in the system. Setting the PSH at the same location as the wind farm, the wind energy curtailment has been reduced significantly. PSH could employ the extra wind energy by pumping water from the lower to upper reservoir and store more water at upper reservoir. When the system requires power, PSH could use hydro turbines to generate power through moving water from the upper to lower reservoir. With a lower wind curtailment in such scenarios, PSH could rapidly supply power for system restoration after absorbing redundant wind energy. Additionally, PSH can operate as BS units to shorten the restoration time.

Wind energy and PSH have positive impact on the system restoration. The system integrating both wind energy and PSH owns a stronger restoration capability. After a blackout occurs, this system not only is restored with high efficiency and more resiliently, but also improves utilization of renewable energy.

6.2 Suggestions for Future Research

In this thesis, the presented model is tested in the cases with stable output of wind energy. However, the output of wind energy is not always stable and the inherent uncertainty and forecast variations may exist. Wind power is hard to be predicted accurately and processes more variability and uncertainty than conventional energy resources. It is suggested to further discuss the impact of wind energy considering

uncertainty. Moreover, other sources of flexibility such as the optimal transmission reconfiguration and topology change could be also considered for the system restoration, collectively help achieving a higher network resilience in the face of HILP events.

Therefore, the future works include two aspects: 1) Develop a real-time optimization model for system restoration considering wind uncertainty; 2) Study the impacts of network topology change for the system restoration.

References

- [1] "Enhancing the Resilience of the Nation's Electricity Systems," The National Academies Series, July 2017.
- [2] R. J. Campbell, "Weather-related Power Outages and Electric System Resiliency," Library of Congress, 2012.
- [3] A. Kenward and U. Raja, "Blackout: Extreme Weather, Climate Change and Power Outages," Climate Central, 2014.
- [4] "Significant Weather-related U.S. Electric Grid Disturbances," Global Climate Change Impacts in the United States Report, 2009. [Online]. Available: <https://nca2009.globalchange.gov/significant-weather-related-us-electric-grid-disturbances/index.html>.
- [5] P. Dehghanian, B. Zhang, T. Dokic and M. Kezunovic, "Predictive Risk Analytics for Weather-resilient Operation of Electric Power System," *IEEE Transactions on Sustainable Energy*, vol. 10, no. 1, pp. 3-15, Jan. 2019.
- [6] P. Dehghanian, "Power System Topology Control for Enhance Resilience of Smart Electricity Grids," Department of Electrical and Computer Engineering, Texas A&M University, College Station, Texas, USA, 2017.
- [7] "Economic Benefits of Increasing Electric Grid Resilience to Weather Outages," Executive Office of President, Aug. 2013.
- [8] "A Methodology for Cost-risk Analysis in the Statistical Validation of Simulation Models," National Climate Data Center, 2012.
- [9] "State of Reliability 2018," North American Electric Reliability Corporation, June 2018.
- [10] Z. Tayebi and B. Najafi, "Determination of vulnerability and risk management in microcredit programs: applying risk sharing model and panel data approach," *Iranian Journal of Agricultural Economics*, vol. 5, no. 4, pp. 25-49, 2012.
- [11] Z. Tayebi and L. E. Fulginiti, "Agricultural productivity and climate change in the greater middle east," 2016.
- [12] Z. Tayebi and G. Onel, "Revisiting the neoclassical model of out-farm migration: Evidence from nonlinear panel time series data," in *Agricultural and Applied Economics Association Annual Meeting*, 2017.

- [13] Z. Tayebi and G. Onel, "Microcredit programs, poverty and vulnerability in rural Iran," in *Southern Agricultural Economics Association Annual Meeting*, 2016.
- [14] Z. Tayebi and M. Bakhshoodeh, "Factors affecting procrastination of rural women's decision making to participate in micro credit funds and self-financed groups in Fars," *Iranian Journal of Rural Economics*, vol. 2, no. 4, pp. 1-14, 2015.
- [15] R. Cormier, "The 12 Biggest Blackouts in History," Nov. 2015. [Online]. Available: <http://mentalfloss.com/article/57769/12-biggest-electrical-blackouts-history>.
- [16] S. Liu, Y. Hou, C. Liu and R. Podmore, "The Healing Touch and Challenges for Smart Grid Restoration," *IEEE Power and Energy Magazine*, vol. 12, no. 1, pp. 54-63, Jan./Feb. 2014.
- [17] M. Nazemi, M. Moeini-Aghtaie, M. Fotuhi-Firuzabad and P. Dehghanian, "Energy Storage Planning for Enhanced Resilience of Power Distribution Networks against Earthquakes," *IEEE Transactions on Sustainable Energy*, Accepted for Publication, in Press, 2019.
- [18] P. Dehghanian, S. Aslan and P. Dehghanian, "Maintaining Electric System Safety through an Enhanced Network Resilience," *IEEE Transactions on Industry Applications*, vol. 54, no. 5, pp. 4927-4937, Sept.-Oct. 2018.
- [19] F. Pourahmadi, H. Heidarabadi, H. Hosseini and P. Dehghanian, "Dynamic Uncertainty Set Characterization for Bulk Power Grid Flexibility Assessment," *IEEE Systems Journal*, Accepted for Publication, in Press, 2019.
- [20] B. Zhang, P. Dehghanian and M. Kezunovic, "Optimal Allocation of PV Generation and Battery Storage for Enhanced Resilience," *IEEE Transactions on Smart Grid*, vol. 10, no. 1, pp. 535-545, Jan. 2019.
- [21] S. Wang, P. Dehghanian and Y. Gu, "A Novel Multi-Resolution Wavelet Transform for Online Power Grid Waveform Classification," in *The 1st IEEE International Conference on Smart Grid Synchronized Measurements and Analytics (SGSMA)*, College Station, Texas, USA, 20-23 May 2019.
- [22] S. Wang, P. Dehghanian, M. Alhazmi, J. Su and B. Shinde, "Resilience-Assured Protective Control of DC/AC Inverters under Unbalanced and Fault Scenarios," in *The 10th IEEE Power and Energy Society (PES) Conference on Innovative Smart Grid Technologies-North America (ISGT-NA)*, Washington, DC, USA, 18-21 Feb. 2019.
- [23] P. Dehghanian, S. Aslan and P. Dehghanian, "Quantifying Power System Resiliency Improvement using Network Reconfiguration," in *IEEE 60th*

International Midwest Symposium on Circuits and Systems (MWSCAS), Boston, MA, USA, 2017.

- [24] M. Kezunovic, P. Dehghanian and J. Sztipanovits, "An Incremental System-of-Systems Integration Modelling of Cyber-Physical Electric Power Systems," in *Grid of the Future Symposium, CIGRE US National Committee*, Philadelphia, Pennsylvania, USA, Oct.-Nov. 2016.
- [25] B. Zhang, P. Dehghanian and M. Kezunovic, "Spatial-Temporal Solar Power Forecast through Gaussian Conditional Random Fields," in *IEEE Power and Energy Society (PES) General Meeting*, Boston, MA, USA, July 2016.
- [26] T. Dokic, P. Dehghanian, P.-C. Chen, M. Kezunovic, Z. Medina-Cetina, J. Stojanovic and Z. Obradovic, "Risk Assessment of a Transmission Line Insulation Breakdown due to Lightning and Severe Weather," in *The 49th Hawaii International Conference on System Science (HICSS)*, Big Island, USA, Jan. 2016.
- [27] B. Zhang, P. Dehghanian and M. Kezunovic, "Simulation of Weather Impacts on the Wholesale Electricity Market," in *10th International Conference on Deregulated Electricity Market Issues in South Eastern Europe (DEMSEE)*, Budapest, Hungary, Sept. 2015.
- [28] "PJM Manual 36: System Restoration," PJM, June 2018. [Online]. Available: <https://www.pjm.com/library/manuals.aspx..>
- [29] L. Slocum, "The Worst Natural Disasters of 2018," Apr. 2019. [Online]. Available: <https://www.ranker.com/list/worst-natural-disasters-2018/lauren-slocum>.
- [30] "Global Wind Report: Annual Market Update 2015," Global Wind Energy Council (GWEC), 2016.
- [31] "20% Wind Energy by 2030: Increasing Wind Energy's Contribution to U.S. Electricity Supply," U.S. Department of Energy, July 2008.
- [32] "Wind Vision: A New Era for Wind Power in the United States," U.S. Department of Energy, 2015.
- [33] "U.S. Wind Industry Annual Market Report 2018," American Wind Energy Association, 2019.
- [34] J. Hetzer, D. C. Yu and K. Bhattarai, "An Economic Dispatch Model Incorporating Wind Power," *IEEE Transactions on Energy Conversion*, vol. 23, no. 2, pp. 603-611, June 2008.

- [35] S. M. Amin and A. M. Giacomoni, "Smart Grid, Safe Grid," *IEEE Power and Energy Magazine*, vol. 10, no. 1, pp. 33-40, Jan./Feb. 2012.
- [36] A. Golshani, W. Sun, Q. Zhou, Q. P. Zhang and Y. Hou, "Incorporating Wind Energy in Power System Restoration Planning," *IEEE Transactions on Smart Grid*, vol. 10, no. 1, pp. 16-28, Jan. 2019.
- [37] S. M. Mohammadi-Hosseininejad, A. Fereidunian, A. Shahavari and H. Lesani, "A Healer Reinforcement Approach to Self-Healing in Smart Grid by PHEVs Parking Lot Allocation," *IEEE Transaction on Industrial Informatics*, vol. 12, no. 6, pp. 2020-2030, Dec. 2016.
- [38] A. Golshani, W. Sun and Q. Zhou, "PHEVs Contribution to the Self-Healing Process of Distribution Systems," in *2016 IEEE Power and Energy Society General Meeting*, July 2016.
- [39] C. P. Nguyen and A. J. Flueck, "Agent Based Restoration with Distributed Energy Storage Support in Smart Grids," *IEEE Transactions on Smart Grid*, vol. 3, no. 2, pp. 1029-1038, June 2012.
- [40] S. Lei, C. Chen, H. Zhou and Y. Hou, "Routing and Scheduling of Mobile Power Sources for Distribution System Resilience Enhancement," *IEEE Transactions on Smart Grid*, 2018.
- [41] "Black Start," Wikipedia, [Online]. Available: https://en.wikipedia.org/wiki/Black_start#cite_note-Knight01-1.
- [42] U. G. Knight, *Power Systems in Emergencies - From Contingency Planning to Crisis Management*, John Wiley & Sons, 2001.
- [43] M. Adibi, P. Clelland, L. Fink, H. Happ, R. Kafka, J. Raine, D. Scheurer and F. Trefny, "Power System Restoration - A Task Force Report," *IEEE Transactions on Power System*, vol. 2, no. 2, pp. 271-277, May 1987.
- [44] M. M. Adibi, *Power System Restoration: Methodologies & Implementation Strategies*, Wiley-IEEE Press, 2000.
- [45] "System Restoration from Blackstart Resources," North American Electric Reliability Corporation, 2009. [Online]. Available: <https://www.nerc.com/pa/Stand/Reliability%20Standards/EOP-005-2.pdf>.
- [46] "System Restoration Coordination," North American Electric Reliability Corporation, 2009. [Online]. Available: <https://www.nerc.com/pa/Stand/Reliability%20Standards/EOP-006-3.pdf>.

- [47] R. J. Kafka, "Review of PJM Restoration Practices and NERC Restoration Standards," in *2008 IEEE Power and Energy Society General Meeting*, 2008.
- [48] W. Sun, C. Liu and L. Zhang, "Optimal Generator Start-up Strategy for Bulk Power System Restoration," *IEEE Transactions on Power Systems*, vol. 26, no. 3, pp. 1357-1366, Aug. 2011.
- [49] W. Sun and C. Liu, "Optimal Transmission Path Search in Power System Restoration," in *2013 IREP Symposium-Bulk Power System and Control - IX(IREP)*, Rethymnon, Greece, Aug. 2013.
- [50] J. Feltes and C. Grande-Moran, "Down, but Not Out: A Brief Overview of Restoration Issues," *IEEE Power and Energy Magazine*, vol. 12, no. 1, pp. 34-43, Jan./Feb. 2014.
- [51] "MISO Power System Restoration Plan," Midcontinent Independent System Operator, Apr. 2019. [Online]. Available: <https://cdn.misoenergy.org/SO-P-PSR-01%20Rev%202%20MISO%20Power%20System%20Restoration%20Plan332945.pdf>.
- [52] "Ontario Power System Restoration Plan," Independent Electricity System Operator, Dec. 2018. [Online]. Available: <http://www.ieso.ca/en/Sector-Participants/System-Reliability/Ontario-Power-System-Restoration-Plan>.
- [53] M. Henderson, E. Rappold, J. Feltes, C. Grande-Moran, D. Durbak and O. Bileya, "Addressing restoration issues for the ISO New England system," in *2012 IEEE Power and Energy Society General Meeting*, San Diego, CA, USA, July 2012.
- [54] Z. Qin, Y. Hou, C. Liu, S. Liu and W. Sun, "Coordinating generation and load pickup during load restoration with discrete load increments and reserve constraints," *IET Generation, Transmission & Distribution*, vol. 9, no. 15, pp. 2437-2446, Nov. 2015.
- [55] A. Stefanov, C. Liu, M. Sfora, M. Eremia and R. Balaurescu, "Decision Support for Restoration of Interconnected Power System Using Tie Lines," *IET Generation, Transmission & Distribution*, vol. 9, no. 11, pp. 1006-1018, 2015.
- [56] H. Zhu, J. Wang, K. Liu, X. Lu, X. Wang, F. Zhang, N. Yang and R. Xian, "Multi-objective Preference Optimization of Unit Restoration During Network Reconstruction Based on DE-EDA," in *2018 China International Conference on Electricity Distribution*, Tianjin, China, Sept. 2018.
- [57] L. Li, M. Zhou, S. Li and Y. Li, "A New Method of Black Start Based on VSC-HVDC," in *2010 International Conference on Computing, Control and Industrial Engineering*, Wuhan, China, 2010.

- [58] M. Liu, G. Liu, S. Liang and X. Qiu, "Selection and Simulation of Black-start Diesel Generating Set in Regional Power Grid," in *2018 China International Conference on Electricity Distribution*, Tianjin, China, Sept. 2018.
- [59] R. Podmore, "Smart Grid Restoration Concepts," in *IEEE PES General Meeting*, Providence, RI, USA, July 2010.
- [60] H. Zhu and Y. Liu, "Aspects of Power System Restoration Considering Wind Farms," in *International Conference on Sustainable Power Generation and Supply*, Hangzhou, China, Sept. 2012.
- [61] A. Miller, E. Muljadi and D. S. Zinger, "A Variable Speed Wind Turbine Power Control," *IEEE Transactions on Energy Conversion*, vol. 12, no. 2, pp. 181-186, June, 1997.
- [62] R. Pena, J. C. Clare and G. M. Asher, "Doubly Fed Induction Generator Using Back-to-Back PWM Converters and Its Application to Variable-speed Wind-energy Generation," *IEE Proceeding - Electric Power Application*, vol. 143, no. 3, pp. 231-241, May 1996.
- [63] M. Aktarujjaman, M. A. Kashem, M. Negnevitsky and G. Ledwich, "Black Start with DFIG Based Distributed Generation after Major Emergencies," in *2006 International Conference on Power Electronic, Drives and Energy Systems*, New Delhi, India, Dec. 2006.
- [64] Y. Tang, J. Dai and Y. Feng, "Frequency Control Strategy for Black Starts via PMSG-Based Wind Power Generation," *Energies*, vol. 10, no. 3, Mar. 2017.
- [65] L. Seca, H. Costa, C. L. Moreira and J. A. Pecas Lopes, "An Innovative Strategy for Power System Restoration Using Utility Scale Wind Parks," in *2013 IREP Symposium Bulk Power System Dynamics and Control - IX Optimization, Security and Control of the Emerging Power Grid*, Rethymno, Greece, Oct. 2013.
- [66] A. M. Ei-Zonkoly, "Renewable Energy Sources for Complete Optimal Power System Black-start Restoration," *IET Generation, Transmission & Distribution*, vol. 9, no. 6, pp. 531-539, Apr. 2015.
- [67] H. Cui, B. Sang, G. Li, A. Hu, B. Yang and Y. Tao, "Research on Method of Photovoltaic Power Station Assisting Power Grid Black Start Based on Energy Storage," in *2018 2nd IEEE Conference on Energy Internet and Energy System Integration (EI2)*, Beijing, China, Oct. 2018.
- [68] P. Dehghanian and M. Kezunovic, "Probabilistic Decision Making for the Bulk Power System Optimal Topology Control," *IEEE Transactions on Smart Grid*, vol. 7, no. 4, pp. 2071-2081, July 2016.

- [69] M. Nazemi, P. Dehghanian and M. Lejeune, "A Mixed-Integer Distributionally Robust Chance-Constrained Model for Optimal Topology Control in Power Grids with Uncertain Renewables," in *13th IEEE Power and Energy Society (PES) PowerTech Conference*, Milan, Italy, 23-27 June 2019.
- [70] M. Alhazmi, P. Dehghanian, S. Wang and B. Shinde, "Power Grid Optimal Topology Control Considering Correlations of System Uncertainties," in *IEEE/IAS 55th Industrial and Commercial Power Systems (I&CPS) Technical Conference*, Calgary, Canada, May 2019.
- [71] P. Dehghanian and M. Kezunovic, "Probabilistic Impact of Transmission Line Switching on Power System Operating States," in *IEEE Power and Energy Society (PES) Transmission and Distribution (T&D) Conference and Exposition*, Dallas, USA, May 2016.
- [72] P. Dehghanian and M. Kezunovic, "Impact Assessment of Power System Topology Control on System Reliability," in *IEEE Conference on Intelligent Systems Applications to Power Systems (ISAP)*, Porto, Portugal, 11-16 Sept. 2015.
- [73] K. W. Hedman, S. S. Oren and R. P. O'Neill, "A Review of Transmission Switching and Network Topology Optimization," in *IEEE Power and Energy Society General Meeting*, Detroit, MI, USA, July 2011.
- [74] G. Poyrazoglu and O. HyungSeon, "Optimal Topology Control with Physical Power Flow Constraints and N-1 Contingency Criterion," *IEEE Transactions on Power Systems*, vol. 30, no. 6, pp. 3063-3071, Nov. 2015.
- [75] A. R. Escobedo, E. Moreno-Centeno and K. W. Hedman, "Topology Control for Load Shed Recovery," *IEEE Transactions on Power System*, vol. 29, no. 2, pp. 908-916, Mar. 2014.
- [76] P. Dehghanian, Y. Wang, G. Gurralla, E. Moreno-Centeno and M. Kezunovic, "Flexible Implementation of Power System Corrective Topology Control," *Electric Power System Research*, vol. 128, pp. 79-89, Nov. 2015.
- [77] M. Kezunovic, T. Popovic, G. Gurralla, P. Dehghanian, A. Esmaeilian and M. Tasdighi, "Reliable Implementation of Robust Adaptive Topology Control," in *The 47th Hawaii International Conference on System Sciences (HICSS)*, Big Island, USA., Jan. 2014.
- [78] H. Weber and M. Krueger, "Dynamic Investigation of Network Restoration by the Pumped-storage Plant Markersbach in Germany," in *The International Federation of Automatic Control*, Seoul, Korea, June 2018.

- [79] J. Lai, X. Lu, F. Wang, P. Dehghanian and R. Tang, "Broadcast Gossip Algorithms for Distributed Peer-to-Peer Control in AC Microgrids," *IEEE Transactions on Industry Applications*, vol. 55, no. 3, pp. 2241-2251, 2019.
- [80] F. Pourahmadi and P. Dehghanian, "A Game-Theoretic Loss Allocation Approach in Power Distribution Systems with High Penetration of Distributed Generations," *Mathematics*, vol. 6, no. 9, pp. 1-14, 2018.
- [81] J. Lai, X. Lu, F. Wang and P. Dehghanian, "Fully-Distributed Gossip Control for Voltage Regulation of Inverter-based DRs in P2P Microgrids," in *IEEE Industry Applications Society (IAS) Annual Meeting*, Portland, Oregon, USA, 2018.
- [82] P. Dehghanian, Y. Guan and M. Kezunovic, "Real-Time Life-Cycle Assessment of High Voltage Circuit Breakers for Maintenance using Online Condition Monitoring Data," *IEEE Transactions on Industry Applications*, vol. 55, no. 2, pp. 1135-1146, Mar.-Apr. 2019.
- [83] P. Dehghanian, M. Fotuhi-Firuzabad, S. Bagheri-Shouraki and A. A. Razi Kazemi, "Critical Component Identification in Reliability Centered Asset Management of Distribution Power Systems via Fuzzy AHP," *IEEE Systems Journal*, vol. 6, no. 4, pp. 593-602, Dec. 2012.
- [84] P. Dehghanian, M. Fotuhi-Firuzabad, F. Aminifar and R. Billinton, "A Comprehensive Scheme for Reliability Centered Maintenance Implementation in Power Distribution Systems- Part II: Numerical Analysis," *IEEE Transactions on Power Delivery*, vol. 28, no. 2, pp. 711-778, Apr. 2013.
- [85] P. Dehghanian, M. Fotuhi-Firuzabad, F. Aminifar and R. Billinton, "A Comprehensive Scheme for Reliability Centered Maintenance Implementation in Power Distribution Systems- Part I: Methodology," *IEEE Transactions on Power Delivery*, vol. 28, no. 2, pp. 761-770, Apr. 2013.
- [86] S. Moradi, V. Vahidinasab, M. Kia and P. Dehghanian, "A Mathematical Framework for Reliability-Centered Asset Management Implementation in Microgrids," *International Transactions on Electrical Energy Systems*, 2018.
- [87] F. Pourahmadi, M. Fotuhi-Firuzabad and P. Dehghanian, "Identification of Critical Generating Units for Maintenance: A Game Theory Approach," *IET Generation, Transmission & Distribution*, vol. 10, no. 12, pp. 2942-2952, 2016.
- [88] R. Ghorani, M. Fotuhi-Firuzabad, P. Dehghanian and W. Li, "Identifying Critical Component for Reliability Centered Maintenance Management of Deregulated Power Systems," *IET Generation, Transmission, and Distribution*, vol. 9, no. 9, pp. 828-837, June 2015.

- [89] H. Sabouhi, M. Fotuhi-Firuzabad and P. Dehghanian, "Identifying Critical Components of Combined Cycle Power Plants for Implementation of Reliability Centered Maintenance," *IEEE CSEE Journal of Power and Energy Systems*, vol. 2, no. 2, pp. 87-97, June 2016.
- [90] H. Sabouhi, A. Abbaspour, M. Fotuhi-Firuzabad and P. Dehghanian, "Reliability Modeling and Availability Analysis of Combined Cycle Power Plants," *International Journal of Electrical Power and Energy Systems*, vol. 79, pp. 108-119, July 2016.
- [91] H. Mirsaedi, A. Fereidunian, S. M. Mohammadi-Hosseininejad, P. Dehghanian and H. Lesani, "Long-Term Maintenance Scheduling and Budgeting in Electricity Distribution Systems Equipped with Automatic Switches," *IEEE Transactions on Industrial Informatics*, vol. 14, no. 5, pp. 1909-1919, May 2018.
- [92] A. Asghari Gharakheili, M. Fotuhi-Firuzabad and P. Dehghanian, "A New Multi-Attribute Support Tool for Identifying Critical Components in Power Transmission Systems," *IEEE Systems Journal*, vol. 12, no. 1, pp. 316-327, Mar. 2018.
- [93] F. Pourahmadi, M. Fotuhi-Firuzabad and P. Dehghanian, "Application of Game Theory in Reliability Centered Maintenance of Electric Power Systems," *IEEE Transactions on Industry Applications*, vol. 53, no. 2, pp. 936-946, Mar.-Apr. 2017.
- [94] P. Dehghanian, Y. Guan and M. Kezunovic, "Real-Time Life-Cycle Assessment of Circuit Breakers for Maintenance using Online Condition Monitoring Data," in *IEEE/IAS 54th Industrial and Commercial Power Systems (I&CPS) Technical Conference*, Niagara Falls, Canada, May 2018.
- [95] F. Pourahmadi, M. Fotuhi-Firuzabad and P. Dehghanian, "Identification of Critical Components in Power Systems: A Game Theory Application," in *IEEE Industry Application Society (IAS) Annual Meeting*, Portland, Oregon, USA, Oct. 2016.
- [96] P. Dehghanian, T. Popovic and M. Kezunovic, "Circuit Breaker Operational Health Assessment via Condition Monitoring Data," in *The 46th North American Power Symposium, (NAPS)*, Pullman, Washington, USA, Sept. 2014.
- [97] P. Dehghanian, M. Moeini-Aghtaie, M. Fotuhi-Firuzabad and R. Billinton, "A Practical Application of the Delphi Method in Maintenance-Targeted Resource Allocation of Distribution Utilities," in *The 13th International Conference on Probabilistic Methods Applied to Power Systems (PMAPS)*, Durham, England, July 2014.
- [98] P. Dehghanian and M. Kezunovic, "Cost/Benefit Analysis for Circuit Breaker Maintenance Planning and Scheduling," in *The 45th North American Power Symposium (NAPS)*, Manhattan, Kansas, USA, Sept. 2013.

- [99] Y. Guan, M. Kezunovic, P. Dehghanian and G. Gurralla, "Assessing Circuit Breaker Life Cycle using Condition-based Data," in *IEEE Power and Energy Society (PES) General Meeting*, Vancouver, British Columbia, Canada, July 2013.
- [100] P. Dehghanian, M. Kezunovic, G. Gurralla and Y. Guan, "Security-Based Circuit Breaker Maintenance Management," in *IEEE Power and Energy Society (PES) General Meeting*, Vancouver, British Columbia, Canada, July 2013.
- [101] P. Dehghanian and M. Fotuhi-Firuzabad, "A Reliability-Oriented Outlook on the Critical Components of Power Distribution Systems," in *The 9th IET International Conference on Advances in Power System Control, Operation, and Management (APSCOM)*, Hong Kong, China, Nov. 2012.
- [102] P. Dehghanian, M. Moeini-Aghtaie, M. Fotuhi-Firuzabad and A. Abbaspour, "Incorporating Probabilistic Cost/Worth Analysis in Maintenance Prioritization of Power Distribution Components," in *12th International Conference on Probabilistic Methods Applied to Power Systems (PMAPS)*, Istanbul, Turkey, June 2012.
- [103] L. Jalili, M. Sadeghi-Khomam, M. Fotuhi-Firuzabad, P. Dehghanian and A. Rajabi-Ghahnavieh, "Designing an Effective and Financially Efficient Risk-Oriented Model for Maintenance Planning of Power Systems: A Practical Perspective," in *12th International Conference on Probabilistic Methods Applied to Power Systems (PMAPS)*, Istanbul, Turkey, June 2012.
- [104] P. Dehghanian, S. H. Hosseini, M. Moeini-Aghtaie and S. Arabali, "Optimal Siting of DG Units in Power Systems from a Probabilistic Multi-Objective Optimization Perspective," *International Journal of Electrical Power and Energy Systems*, vol. 51, pp. 14-26, Oct. 2013.
- [105] A. A. Razi Kazemi and P. Dehghanian, "A Practical Approach to Optimal RTU Placement in Power Distribution Systems Incorporating Fuzzy Sets Theory," *International Journal of Electrical Power and Energy Systems*, vol. 37, no. 1, pp. 31- 42, May 2012.
- [106] A. S. Arabali, P. Dehghanian, M. Moeini-Aghtaie and A. Abbaspour, "The Impact of Dispersed PV Generation on Ramp Rate Requirements," in *11th International IEEE Conference on Electrical and Environmental Engineering (EEEIC)*, Venice, Italy, May 2012.
- [107] H. Sarparandeh, M. Moeini-Aghtaie, P. Dehghanian, I. Harsini and A. Haghani, "Feasibility Study of Operating An Autonomous Power System in Presence of Wind Turbines - A Practical Experience in Manjil, Iran," in *11th International IEEE*

Conference on Electrical and Environmental Engineering (EEEIC), Venice, Italy, May 2012.

- [108] M. Shojaei, V. Rastegar-Moghaddam, A. Razi Kazemi, P. Dehghanian and G. Karami, "A New Look on the Automation of Medium Voltage Substations in Power Distribution Systems," in *17th Conference on Electric Power Distribution Networks (EPDC)*, Tehran, Iran, May 2012.
- [109] P. Dehghanian, A. A. Razi Kazemi and G. Karami, "Incorporating Experts Knowledge in RTU Placement Procedure Using Fuzzy Sets Theory- A Practical Approach," in *The 33rd IEEE International Telecommunications Energy Conference (INTELEC)*, Amsterdam, Netherlands, Oct. 2011.
- [110] A. A. Razi Kazemi, P. Dehghanian and G. Karami, "A Probabilistic Approach for Remote Terminal Unit Placement in Power Distribution Systems," in *The 33rd IEEE International Telecommunications Energy Conference (INTELEC)*, Amsterdam, Netherlands, Oct. 2011.
- [111] M. Moeini-Aghtaie, P. Dehghanian and S. H. Hosseini, "Optimal Distributed Generation Placement in a Restructured Environment via a Multi-Objective Optimization Approach," in *16th Conference on Electric Power Distribution Networks (EPDC)*, Bandar-Abbas, Iran, May 2011.
- [112] P. Dehghanian, A. A. Razi Kazemi and M. Fotuhi-Firuzabad, "Optimal RTU Placement in Power Distribution Systems Using a Novel Method Based on Analytical Hierarchical Process (AHP)," in *The 10th International IEEE Conference on Environmental and Electrical Engineering (EEEIC)*, Rome, Italy, May 2011.
- [113] M. A. Saffari, M. S. Misaghian, M. Kia, A. Heidari, P. Dehghanian and J. Aghaei, "Robust/Stochastic Optimization of Energy Arbitrage in Smart Microgrids using Electric Vehicles," *Electric Power Systems Research*, Accepted for Publication, in Press, 2019. .
- [114] B. Wang, J. A. Camacho, G. M. Pulliam, A. H. Etemadi and P. Dehghanian, "New Reward and Penalty Scheme for Electric Distribution Utilities Employing Load-Based Reliability Indices," *IET Generation, Transmission & Distribution*, vol. 12, no. 15, pp. 3647-2654, 2018.
- [115] M. Moeini-Aghtaie, A. Abbaspour, M. Fotuhi-Firuzabad and P. Dehghanian, "Optimized Probabilistic PHEV Demand Management in the Context of Energy Hubs," *IEEE Transactions on Power Delivery*, vol. 30, no. 2, pp. 996-1006, Apr. 2015.

- [116] M. Moeini-Aghaie, P. Dehghanian, M. Fotuhi-Firuzabad and A. Abbaspour, "Multi-Agent Genetic Algorithm: An Online Probabilistic View on Economic Dispatch of Energy Hubs Constrained by Wind Availability," *IEEE Transactions on Sustainable Energy*, vol. 5, no. 2, pp. 669-708, Apr. 2014.
- [117] A. Mukhatov, M. Bagheri, P. Dehghanian, V. Carabias and G. B. Gharehpetian, "Reduction of Output Power Pulsations for Electric Vehicles by Changing Distances Between Transmitter Coils," in *The 7th International Conference on Renewable Energy Research and Applications (ICREA)*, Paris, France, Oct. 2018.
- [118] M. S. Misaghian, M. Safari, A. Heidari, A. Kia, P. Dehghanian and B. Wang, "Electric Vehicles Contributions to Voltage Improvement and Loss Reduction in Microgrids," in *The 50th North American Power Symposium (NAPS)*, Fargo, North Dakota, USA, Sept. 2018.
- [119] M. Moeini-Aghaie, A. Abbaspour, M. Fotuhi-Firuzabad and P. Dehghanian, "PHEV's Centralized/Decentralized Charging Control Mechanisms: Requirements and Impacts," in *The 45th North American Power Symposium (NAPS)*, Manhattan, Kansas, USA, Sept. 2013.
- [120] T. Becejac and P. Dehghanian, "PMU Multilevel End-to-End Testing to Assess Synchrophasor Measurements during Faults," *IEEE Power and Energy Technology Systems Journal*, vol. 6, no. 1, pp. 71-80, Mar. 2019.
- [121] S. Wang, L. Li and P. Dehghanian, "Power Grid Online Surveillance through PMU-Embedded Convolutional Neural Networks," in *IEEE Industry Applications Society (IAS) Annual Meeting*, Baltimore, Maryland, USA, Sept.-Oct. 2019.
- [122] S. Wang, P. Dehghanian and B. Zhang, "A Data-Driven Algorithm for Online Power Grid Topology Change Identification with PMUs," in *IEEE Power and Energy Society (PES) General Meeting*, Atlanta, Georgia, USA, Aug. 2019.
- [123] M. H. Rezaeian Koochi, P. Dehghanian, S. Esmaili, P. Dehghanian and S. Wang, "A Synchrophasor-based Decision Tree Approach for Identification of Most Coherent Generating Units," in *The 44th Annual Conference of the IEEE Industrial Electronics Society (IECON)*, Washington DC, USA, Oct. 2018.
- [124] T. Becejac, P. Dehghanian and M. Kezunovic, "Impact of PMU Errors on the Synchrophasor-based Fault Location Algorithms," in *48th North American Power Symposium (NAPS)*, Denver, Colorado, USA, Sept. 2016.
- [125] T. Becejac, P. Dehghanian and M. Kezunovic, "Probabilistic Assessment of PMU Integrity for Planning of Periodic Maintenance and Testing," in *International Conference on Probabilistic Methods Applied to Power Systems (PMAPS)*, Beijing, China, Oct. 2016.

- [126] T. Becejac, P. Dehghanian and M. Kezunovic, "Analysis of PMU Algorithm Errors During Fault Transients and Out-of-Step Disturbances," in *IEEE Power and Energy Society (PES) Transmission & Distribution (T&D) Conference and Exposition Latin America*, Morelia, Mexico, Sept. 2016.
- [127] M. Kezunovic, A. Esmaeilian, T. Becejac, P. Dehghanian and C. Qian, "Life-Cycle Management Tools for Synchrophasor Systems: Why We Need Them and What They Should Entail," in *The 2016 IFAC CIGRE/CIRED Workshop on Control of Transmission and Distribution Smart Grids*, Czech Republic, Oct. 2016.
- [128] H. Zhang, G. T. Heydt, V. Vittal and J. Quintero, "An Improved Network Model for Transmission Expansion Planning Considering Reactive Power and Network Losses," *IEEE Transactions on Power Systems*, vol. 28, no. 3, pp. 3471-3479, Aug. 2013.
- [129] "Pumped-Storage Hydropower," U.S. Department of Energy, [Online]. Available: <https://www.energy.gov/eere/water/pumped-storage-hydropower>.
- [130] R. Uria-Martinez, P. O'Connor and M. Johnson, "2014 Hydropower Market Report," U.S. Department of Energy, Washington, D.C., U.S., 2015.
- [131] "Hydropower Vision: A New Chapter for America's 1st Renewable Electricity Source," U.S. Department of Energy, July, 2016.
- [132] A. J. Conejo, J. M. Arroyo, J. Contreras and F. A. Villamor, "Self-scheduling of a Hydro Producer in a Pool-based Electricity Market," *IEEE Transactions on Power Systems*, vol. 17, no. 4, pp. 1265-1272, Nov. 2002.
- [133] A. Golshani, W. Sun, Q. Zhou, Q. Zheng, J. Wang and F. Qiu, "Coordination of Wind Farm and Pumped-Storage Hydro for a Self-Healing Power Grid," *IEEE Transactions on Sustainable Energy*, vol. 9, no. 4, pp. 1910-1920, Oct. 2018.
- [134] M. E. Khodayar, M. Shahidehpour and L. Wu, "Enhancing the Dispatchability of Variable Wind Generation by Coordination with Pumped-Storage Hydro Units in Stochastic Power Systems," *IEEE Transactions on Power Systems*, vol. 28, no. 3, pp. 2808-2818, Aug. 13.
- [135] "IEEE 57-Bus Data.," [Online]. Available: <http://icseg.iti.illinois.edu/ieee-57-bus-system>.

Appendix 1: Linearized AC Power Flow Model

This model is presented in the paper [128]. If the effect of phase shifters and off-nominal transformer turns ratios are neglected, the AC power flow in transmission line k between buses i and j is presented as follows:

$$P_k = V_i^2 g_k - V_i V_j (g_k \cos \theta_k + b_k \sin \theta_k) \quad (1a)$$

$$Q_k = -V_i^2 (b_k + b_{k0}) + V_i V_j (b_k \cos \theta_k - g_k \sin \theta_k) \quad (1b)$$

The linearization of the AC power flow equations is essentially based on a Taylor series and the following assumptions are taken:

- 1) The bus voltage magnitudes are always close to 1.0 per unit (p.u.).
- 2) The angle difference across a line is small so that $\sin \theta_k \approx \theta_k$ and $\cos \theta_k \approx 1$ can be applied.

Based on these two assumptions, the AC power flow equations can be written as:

$$P_k \approx (1 + 2\Delta V_i) g_k - (1 + \Delta V_i + \Delta V_j)(g_k + b_k \theta_k) \quad (2a)$$

$$Q_k \approx -(1 + 2\Delta V_i)(b_k + b_{k0}) + (1 + \Delta V_i + \Delta V_j)(b_k - g_k \theta_k) \quad (2b)$$

Where, $\Delta V^{\min} \leq \Delta V_i \leq \Delta V^{\max}$ is expected to be small. However, (2a) and (2b) still contain nonlinearities. Since ΔV_i , ΔV_j and θ_k are expected to be small, the product $\Delta V_i \theta_k$ and $\Delta V_j \theta_k$ can be treated as second order terms and therefore negligible. Thus, the linearized AC power flow equations are obtained as follows:

$$P_k = (\Delta V_i - \Delta V_j) g_k - b_k \theta_k \quad (3a)$$

$$Q_k = -(1 + 2\Delta V_i) b_{k0} - (\Delta V_i - \Delta V_j) b_k - g_k \theta_k \quad (3b)$$

Where, ΔV_i denotes the voltage magnitude deviation from 1 p.u. at bus i , and θ_k represents phase angle difference across transmission line k . Parameters b_k and b_{k0} are series admittance of transmission line k and shunt admittance of transmission line k , while parameter g_k is conductance of the transmission line k . P_k and Q_k are real and reactive power flow in transmission line k .

Appendix 2: Data of IEEE 57 Bus System

The data of the studied IEEE 57-bus test system is presented in Table 12 to 14 [135].

Table 12 Generator Characteristics

Gen. No.	Pmax (MW)	Pmin (MW)	Qmax (MVar)	Qmin (MVar)	P_g^{start} (MW)	Ramp Rate (MW/min)	Connected Bus No.	T_s (p.u.)
G1	575	0	200	-140	0	5	1	1
G2	100	0	50	-17	1	5	2	6
G3	140	0	60	-10	5	5	3	6
G4	100	0	25	-8	8	5	6	3
G5	550	0	200	-140	6	10	8	12
G6	100	0	9	-3	6	5	9	3
G7	410	0	155	-150	7	10	12	12

Table 13 Load Data and Priorities

Load Bus	P_d^{max} (MW)	Q_d^{max} (MVar)	Priority	Load Bus	P_d^{max} (MW)	Q_d^{max} (MVar)	Priority
1	55.0	17	0.9	29	17.0	2.6	0.9
2	3.0	88	1.0	30	3.6	1.8	1.0
3	41.0	21	1.0	31	5.8	2.9	1.0
5	13.0	4	1.0	32	1.6	0.8	0.8
6	75.0	2	0.8	33	3.8	1.9	1.0
8	150.0	22	1.0	35	6.0	3	0.8
9	121.0	26	1.0	38	14.0	7	0.9
10	5.0	2	0.8	41	6.3	3	1.0
12	377.0	24	0.9	42	7.1	4.4	1.0
13	18.0	2.3	0.8	43	2.0	1	1.0
14	10.5	5.3	0.8	44	12.0	1.8	1.0
15	22.0	5	1.0	47	29.7	11.6	0.8
16	43.0	3	0.8	49	18.0	8.5	1.0
17	42.0	8	0.9	50	21.0	10.5	1.0
18	27.2	9.8	1.0	51	18.0	5.3	1.0
19	3.0	0.6	0.9	52	4.9	2.2	1.0
20	2.3	1	1.0	53	20.0	10	1.0
23	6.3	2.1	1.0	54	4.1	1.4	0.8
25	6.3	3.2	1.0	55	6.8	3.4	1.0
27	9.3	0.5	1.0	56	7.6	2.2	1.0
28	4.6	2.3	1.0	57	6.7	2	0.8

Table 14 Transmission Lines Data

Line No.	From Bus	To Bus	R (p.u.)	X (p.u.)	B (p.u.)
1	1	2	0.0083	0.028	0.129
2	2	3	0.0298	0.085	0.0818
3	3	4	0.0112	0.0366	0.038
4	4	5	0.0625	0.132	0.0258
5	4	6	0.043	0.148	0.0348
6	6	7	0.02	0.102	0.0276
7	6	8	0.0339	0.173	0.047
8	8	9	0.0099	0.0505	0.0548
9	9	10	0.0369	0.1679	0.044
10	9	11	0.0258	0.0848	0.0218
11	9	12	0.0648	0.295	0.0772
12	9	13	0.0481	0.158	0.0406
13	13	14	0.0132	0.0434	0.011
14	13	15	0.0269	0.0869	0.023
15	1	15	0.0178	0.091	0.0988
16	1	16	0.0454	0.206	0.0546
17	1	17	0.0238	0.108	0.0286
18	3	15	0.0162	0.053	0.0544
19	4	18	0	0.555	0
20	4	18	0	0.43	0
21	5	6	0.0302	0.0641	0.0124
22	7	8	0.0139	0.0712	0.0194
23	10	12	0.0277	0.1262	0.0328
24	11	13	0.0223	0.0732	0.0188
25	12	13	0.0178	0.058	0.0604
26	12	16	0.018	0.0813	0.0216
27	12	17	0.0397	0.179	0.0476
28	14	15	0.0171	0.0547	0.0148
29	18	19	0.461	0.685	0
30	19	20	0.283	0.434	0
31	21	20	0	0.7767	0
32	21	22	0.0736	0.117	0
33	22	23	0.0099	0.0152	0
34	23	24	0.166	0.256	0.0084
35	24	25	0	1.182	0
36	24	25	0	1.23	0
37	24	26	0	0.0473	0
38	26	27	0.165	0.254	0
39	27	28	0.0618	0.0954	0
40	28	29	0.0418	0.0587	0

41	7	29	0	0.0648	0
42	25	30	0.135	0.202	0
43	30	31	0.326	0.497	0
44	31	32	0.507	0.755	0
45	32	33	0.0392	0.036	0
46	34	32	0	0.953	0
47	34	35	0.052	0.078	0.0032
48	35	36	0.043	0.0537	0.0016
49	36	37	0.029	0.0366	0
50	37	38	0.0651	0.1009	0.002
51	37	39	0.0239	0.0379	0
52	36	40	0.03	0.0466	0
53	22	38	0.0192	0.0295	0
54	11	41	0	0.749	0
55	41	42	0.207	0.352	0
56	41	43	0	0.412	0
57	38	44	0.0289	0.0585	0.002
58	15	45	0	0.1042	0
59	14	46	0	0.0735	0
60	46	47	0.023	0.068	0.0032
61	47	48	0.0182	0.0233	0
62	48	49	0.0834	0.129	0.0048
63	49	50	0.0801	0.128	0
64	50	51	0.1386	0.22	0
65	10	51	0	0.0712	0
66	13	49	0	0.191	0
67	29	52	0.1442	0.187	0
68	52	53	0.0762	0.0984	0
69	53	54	0.1878	0.232	0
70	54	55	0.1732	0.2265	0
71	11	43	0	0.153	0
72	44	45	0.0624	0.1242	0.004
73	40	56	0	1.195	0
74	56	41	0.553	0.549	0
75	56	42	0.2125	0.354	0
76	39	57	0	1.355	0
77	57	56	0.174	0.26	0
78	38	49	0.115	0.177	0.003
79	38	48	0.0312	0.0482	0
80	9	55	0	0.1205	0

Appendix 3: Data of Pumped-Storage Hydro

The data of the considered Pumped-Storage hydro is shown in Table 15 [133].

Table 15 PSH Units' Characteristics

Parameter	Value	Parameter	Value
$P_h^{g,\max}$	180 (MW)	q_h^{\max}	0.75 (Hm^3 / hr)
$P_h^{g,\min}$	16 (MW)	q_h^{\min}	0.05 (Hm^3 / hr)
$P_h^{p,\max}$	250 (MW)	Vol^{\max}	10 (Hm^3)
$P_h^{p,\min}$	20 (MW)	Vol^{\min}	3 (Hm^3)